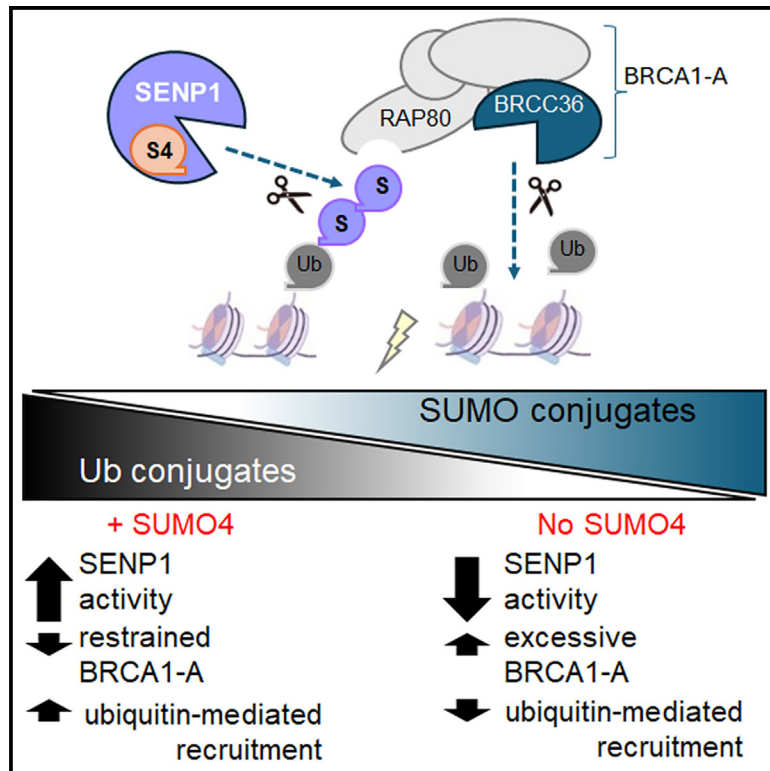


# SUMO4 promotes SUMO deconjugation required for DNA double-strand-break repair

## Graphical abstract



## Authors

Alexander J. Garvin, Alexander J. Lanz, George E. Ronson, ..., Jai S. Bhachoo, Aneika C. Leney, Joanna R. Morris

## Correspondence

a.garvin@leeds.ac.uk (A.J.G.), j.morris.3@bham.ac.uk (J.R.M.)

## In brief

Garvin et al. find that the poorly explored SUMO isoform, SUMO4, enhances the deSUMOylation activity of the SUMO protease SENP1. Consequently, SUMO4 acts to restrain excessive cellular SUMOylation. In the DNA damage response, this activity prevents excessive recruitment of the SUMO-binding protein RAP80 to damage sites and promotes DNA repair.

## Highlights

- The roles of the SUMO family members, SUMO1–4, in DSB repair are not redundant
- SUMO4 conjugation is deleterious
- SUMO4 promotes SENP1 catalytic activity
- SUMO4:SENP1 restrict SUMO signaling and accumulation of the BRCA1-A complex



## Article

# SUMO4 promotes SUMO deconjugation required for DNA double-strand-break repair

Alexander J. Garvin,<sup>1,2,\*</sup> Alexander J. Lanz,<sup>1</sup> George E. Ronson,<sup>1</sup> Matthew J.W. Mackintosh,<sup>1,3</sup> Katarzyna Starowicz,<sup>1,4</sup> Alexandra K. Walker,<sup>1</sup> Yara Aghabi,<sup>1</sup> Hannah MacKay,<sup>1</sup> Ruth M. Densham,<sup>1</sup> Jai S. Bhachoo,<sup>2</sup> Aneika C. Leney,<sup>3</sup> and Joanna R. Morris<sup>1,5,\*</sup>

<sup>1</sup>Birmingham Centre for Genome Biology and Department of Cancer and Genomic Sciences, School of Medicine, College of Medicine and Health, University of Birmingham, Birmingham B15 2TT, UK

<sup>2</sup>SUMO Biology Laboratory, School of Molecular and Cellular Biology, Faculty of Biological Sciences, University of Leeds, Leeds LS2 9JT, UK

<sup>3</sup>School of Biosciences, College of Life and Environmental Sciences, University of Birmingham, Birmingham B15 2TT, UK

<sup>4</sup>Present address: adthera bio, Lyndon House, 62 Hagley Road, Birmingham B16 8PE, UK

<sup>5</sup>Lead contact

\*Correspondence: [a.garvin@leeds.ac.uk](mailto:a.garvin@leeds.ac.uk) (A.J.G.), [j.morris.3@bham.ac.uk](mailto:j.morris.3@bham.ac.uk) (J.R.M.)

<https://doi.org/10.1016/j.molcel.2025.02.004>

## SUMMARY

The amplitudes of small-modifier protein signaling through ubiquitin and the small ubiquitin-like modifiers, SUMO1–3, are critical to the correct phasing of DNA repair protein accumulation, activity, and clearance and for the completion of mammalian DNA double-strand-break (DSB) repair. However, how SUMO-conjugate signaling in the response is delineated is poorly understood. At the same time, the role of the non-conjugated SUMO protein, SUMO4, has remained enigmatic. Here, we reveal that human SUMO4 is required to prevent excessive DNA-damage-induced SUMOylation and deleterious over-accumulation of RAP80. Mechanistically we show that SUMO4 acts independently of its conjugation and potentiates SENP1 catalytic activity. These data identify SUMO4 as a SUMO deconjugation component and show that SUMO4:SENP1 are critical regulators of DNA-damage-induced SUMO signaling.

## INTRODUCTION

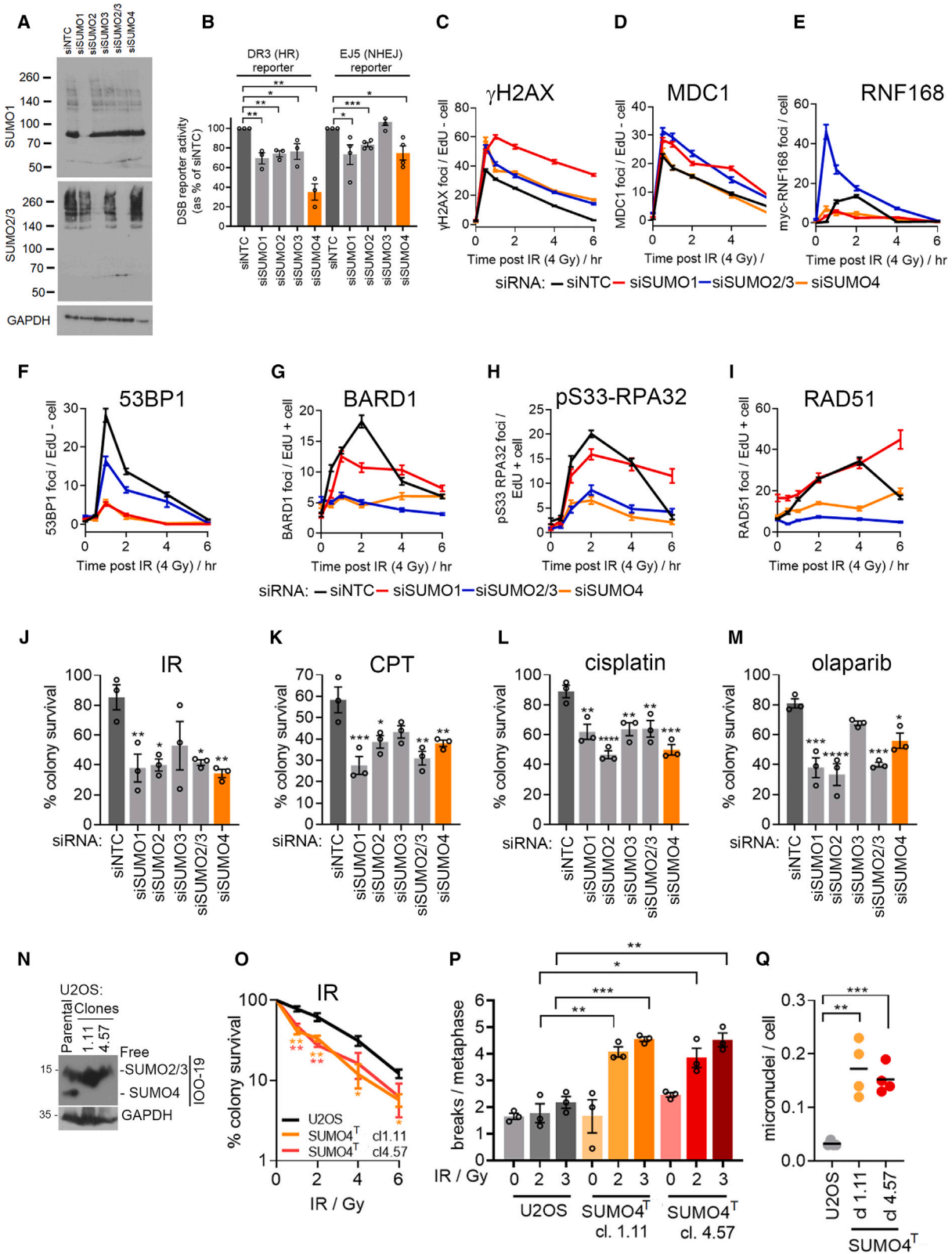
DNA double-strand breaks (DSBs) are severely toxic genomic lesions. Our cells have evolved the means to signal DNA breaks to launch appropriate pathways to repair these lesions. DSBs induce histone modifications and a recruitment cascade of repair proteins regulated by histone and repair protein modifications of phosphorylation, acetylation, methylation, ubiquitination, and the conjugation of small ubiquitin-like modifiers, SUMO1–3 (SUMOylation). The sequencing, duration, and amplitude of post-translational modification signals in the response are critical to directing both a favorable environment for repair and the correct recruitment of repair proteins.

SUMO protein paralogs include SUMO2 and SUMO3, which share 95% identity (hereafter SUMO2/3), and SUMO1, which shares 48% and 46% identity with SUMO2 and SUMO3, respectively.<sup>1</sup> A fourth SUMO protein, SUMO4 has 86% homology to SUMO2, and antibodies that detect SUMO4 cross-react with SUMO2/3 across a range of detection formats.<sup>2</sup> The *SUMO4* gene is a retrogene; its mRNA has been identified by ribosome-profiling across many cell types at folds lower than *SUMO2* or *SUMO3* mRNAs.<sup>3</sup> Nevertheless, proteomics studies have identified unique SUMO4 sequences, including “ANEKP-TEEVKTENNNHINLK” and “TENNNHINLK” (SUMO4-specific

amino acids in bold), confirming its presence *in vivo*.<sup>4–6</sup> Inactive precursors of SUMOs are matured by SENP-specific proteases (SENPs) to expose the di-glycine C-terminal motif required for conjugation.<sup>7</sup> SUMO4 contains a C-terminal proline reported to suppress maturation.<sup>8</sup> Some reports indicate that SUMO4 is not conjugated,<sup>8</sup> whereas others suggest conjugation<sup>9–11</sup> and the possibility that it is matured by non-SENP enzymes,<sup>9</sup> so the relevance of SUMO4 to cellular biology is currently enigmatic. Conjugation of SUMOs to the  $\epsilon$ -amino groups of target lysines commonly uses a three-enzyme cascade (E1-E2-E3) analogous to the enzyme architecture for ubiquitin modification.<sup>12</sup> For many substrates, SUMOylation is highly dynamic. Conjugate liability is due in part to the rapid isopeptidase activity of SENP1-3 and SENP5-7 proteins.<sup>13</sup> A small number of non-SENP deSUMOylating enzymes have also been identified.<sup>14,15</sup>

The balance between SUMOylation and deSUMOylation is altered by exposure to environmental or metabolic stresses, including DSBs.<sup>16–20</sup> The mammalian SUMO E3 ligases PIAS1, PIAS4, and CBX4 drive SUMOylation induced by DNA breaks,<sup>17,21–23</sup> with some indications that SUMO1 conjugation predominates early in the DSB signaling cascade and SUMO2/3 later.<sup>20,21,23</sup> SUMOylation, in large part, acts by increasing interactions between SUMOylated factors and the SUMO-interacting domains (SIMs and other interfaces<sup>24–27</sup>) of partner





(legend on next page)

proteins, which can include SUMO-targeting ubiquitin ligases (StUbls), leading to extraction and degradation of modified proteins.<sup>28–32</sup> Thus, deSUMOylation, for example, of MDC1, restricts StUbl access and regulates the duration of MDC1 localization and, in turn, DSB signaling.<sup>33</sup> Consistent with the proposed role of SUMO as a “molecular glue,”<sup>32,34,35</sup> SUMOylation at DSBs also drives the recruitment of various proteins,<sup>36–42</sup> including the BRCA1-A complex.<sup>43,44</sup>

Here, we compare the influence of each SUMO protein on DSB signaling, finding that each, surprisingly including SUMO4, has distinct roles in the DSB response. We identified SUMO4 as a deconjugation component of the SUMO system, finding that it promotes SENP1 deSUMOylase activity and, consequently, is required to limit SUMOylation. Our data indicate that SUMO4:SENP1 has no influence on SUMOylation/deSUMOylation regulating MDC1 but acts to suppress SUMOylation directed by PIAS1, responsible for RAP80 recruitment, providing further evidence of separable phases of SUMO DSB signaling in mammalian cells. SUMO4 is consequently required for DNA repair, genome stability, and responses to genotoxic stress. Thus, SUMO4 is critical to correct SUMO-signaling amplitude following DSB generation and for promoting DNA repair.

## RESULTS

### SUMO proteins are non-redundant in DSB repair, and SUMO4 plays a distinct role

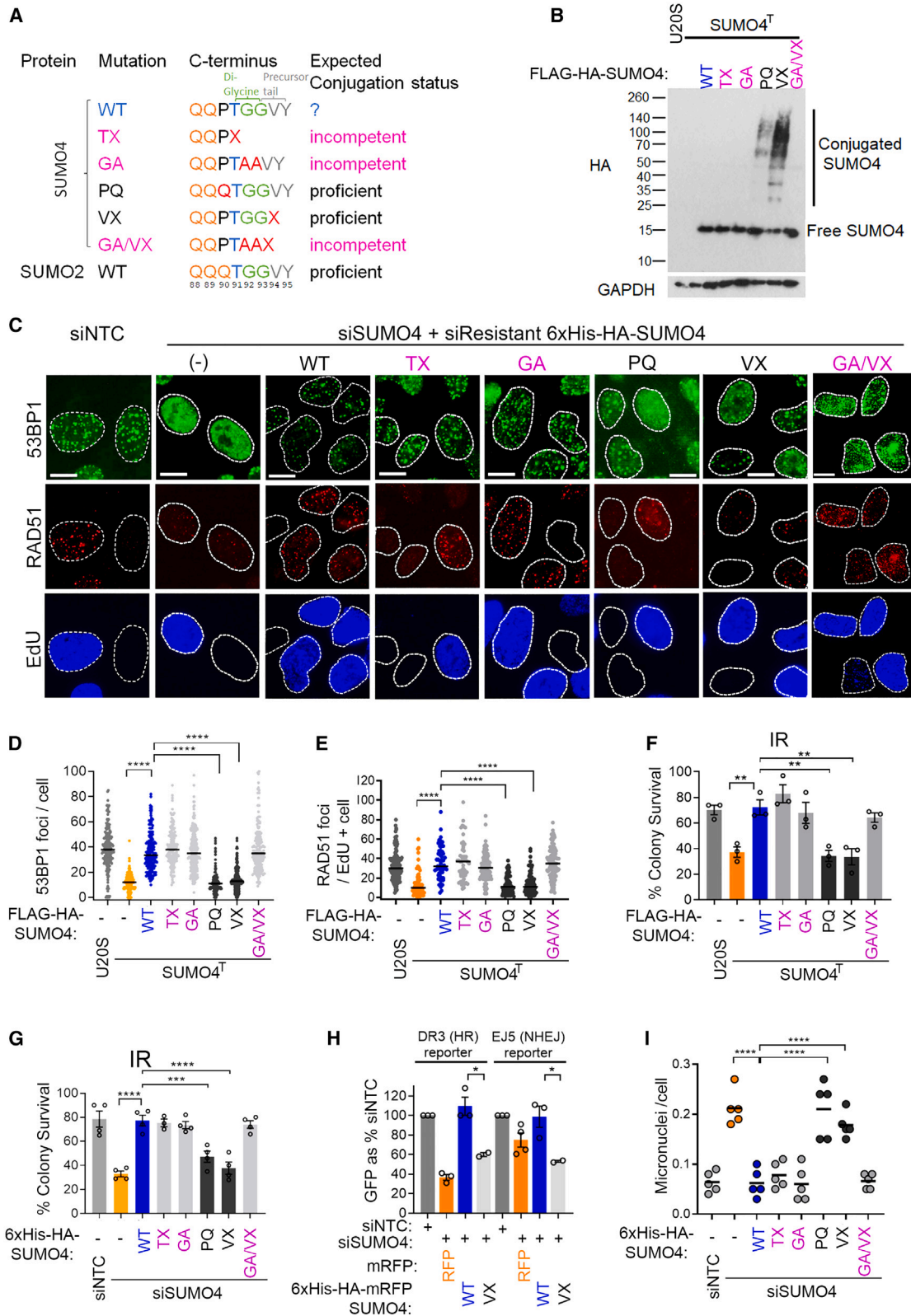
To compare SUMO proteins, we generated small interfering (siRNA) sequences specifically targeting each, including SUMO4 (Figures 1A and S1A). Many antibodies raised to SUMO4 cross-react with SUMO2 and SUMO3, and most of the signal discerned by these antibodies is due to SUMO2/3.<sup>2</sup> We were able to precipitate exogenous SUMO4 slightly better than exogenous SUMO3 when both proteins were highly expressed using one of these antibodies, IOO-19 (Figure S1B), and liquid chromatography-mass spectrometry (LC-MS) of immunoprecipitated endogenous proteins revealed SUMO4-specific peptides (Figures S1C–S1E). A SUMO4 siRNA-sensitive

band was discernible by western blot (Figure S1F), and expression of exogenous 6xHis-HA-SUMO4 in U2OS cells was suppressed by SUMO4 siRNA (Figure S1G). These data indicate SUMO4 siRNA suppresses SUMO4 protein expression. SUMO4 is located within the final intron of the *TAB2* (*MAP3K7IP2*) gene and TAB2 itself has a reported signaling role in DSB repair.<sup>45</sup> Importantly we noted that SUMO4 siRNAs had little impact on TAB2 protein expression (Figure S1H). Next, we compared the effects of different SUMO siRNAs on cell proliferation and cycle distribution of U2OS cells. In contrast to SUMO1 or SUMO2 siRNA treatment, SUMO4 siRNA did not result in a significant decrease in cell number (Figure S1I), and SUMO4 siRNA slightly increased the proportion of cells in S phase over G1 (Figure S1J). We tested DNA repair outcomes of integrated reporters for homologous recombination (gene conversion) and non-homologous end-joining, noting that all SUMO siRNAs, except that to SUMO3, reduced repair outcomes (Figure 1B). SUMO1–4 siRNA treatment also delayed clearance of phosphorylated serine-139 H2AX ( $\gamma$ H2AX) foci following exposure to ionizing irradiation (IR) in both cells pulsed with the nucleotide analog, 5-ethynyl-2'-deoxyuridine (EdU) (S-phase) and EdU negative U2OS cells (Figures 1C and S1K).

Next, we assayed DSB repair protein foci kinetics in SUMO-depleted U2OS cells treated with IR, first assessing MDC1, a repair factor that requires SUMOylation for clearance from DSBs in G1.<sup>28–30,33,36</sup> MDC1 foci resolution was delayed following the depletion of SUMO1 or SUMO2/3 but was unaffected by SUMO4 siRNA (Figure 1D). In contrast, the foci formation of the ubiquitin E3 ligase RNF168 was suppressed in SUMO1- and SUMO4-depleted cells, and SUMO2/3 depletion resulted in excessive RNF168 accrual, particularly at early time points (Figure 1E). When we assessed the recruitment of two downstream readers of the RNF168-generated N-terminally ubiquitinated H2A, 53BP1, and BARD1,<sup>46–48</sup> we found that both were reduced after SUMO4 depletion (Figures 1F, 1G, and S1L). We then tested RPA32 pSer33 foci as an indication of DNA end-resection<sup>49</sup> and RAD51 foci as an indication of the generation of homologous recombination intermediates. Treatment with SUMO4 and SUMO2/3 siRNA reduced both markers

#### Figure 1. SUMO4 is required for DSB repair

- (A) Immunoblot of lysates after treatment with NTC, non-targeting/luciferase, or SUMO siRNAs. SUMO1–4 were each targeted by two siRNA sequences, si-SUMO2/3 used SUMO2 and SUMO3 sequences.
- (B) Homologous recombination (HR) or non-homologous end-joining (NHEJ) reporter cells treated with the indicated siRNAs.  $N = 3$  (HR)  $n = 4$  (NHEJ) experimental repeats. Data are mean  $\pm$  SEM from three independent repeat. Statistical significance: two-tailed t test between siNTC and siSUMO.
- (C)  $\gamma$ H2AX foci in cells treated with indicated siRNA and IR (4 Gy) and fixed at the indicated times.  $N = \sim 150$  cells from  $>100$  cells per condition. Data are mean  $\pm$  SEM.
- (D–I) (D) MDC1 foci, (E) Myc-RNF168 foci, (F) 53BP1 foci, (G) BARD1 foci, (H) RPA32 phospho-S33 foci, and (I) RAD51 foci in cells treated with the indicated siRNA and IR (4 Gy) and fixed at the indicated times. Data are mean  $\pm$  SEM from  $>100$  cells per observation.
- (J–M) Cell survival colony assay (hereafter “colony assay”) following siRNA treatment and (J) 2 Gy IR, (K) 1  $\mu$ M camptothecin (CPT), (L) 1  $\mu$ M cisplatin, and (M) 10  $\mu$ M olaparib. Data are mean  $\pm$  SEM from three independent experiments. Statistical significance: two-tailed t test between siNTC and siSUMO.
- (N) Immunoblot of lysates from parental and SUMO4 edited U2OS clones, cl.1.11 (gRNA #1) and cl.4.57 (gRNA #4) probed with anti-SUMO2/3/4 monoclonal IOO-19 or GAPDH.
- (O) Colony assay of parental and SUMO4<sup>T</sup> cl.1.11 (gRNA #1) and cl.4.57 (gRNA #4) treated with IR at the indicated doses. Data are mean  $\pm$  SEM from three independent experiments. Statistical analysis: two-tailed t test.
- (P) Number of breaks (chromatid and chromosome) per metaphase from three independent experiments in untreated cells or in cells analyzed 24 h after exposure to 2 or 3 Gy IR. Data are mean  $\pm$  SEM from four independent experiments. Statistical significance: two-tailed t test.
- (Q) Micronuclei per cell from 4 independent repeats of IR-treated (4 Gy, fixed 6 h later) parental U2OS<sup>FlpIn</sup> and SUMO4<sup>T</sup> clones 1.11 and 4.57. Data are mean  $\pm$  SEM from four independent experiments 100 nuclei per observation.
- See also Figure S1.



(legend on next page)

following IR (Figures 1H and 1I). In the assessment of the responses to genotoxic agents, depletion of each SUMO isoform (with the exception of SUMO3, after IR or olaparib) increased cell sensitivity to IR, camptothecin (CPT), cisplatin, and the PARP1/2 inhibitor, olaparib (Figures 1J–1M). These data confirm the non-redundant roles of SUMO1 and SUMO2/3 in the DNA damage response and show that SUMO4 targeting impacts DSB signaling in a distinct manner.

To explore the role of SUMO4 further, we tested SUMO4 siRNA treatment of HeLa and NCI-H1299 cells and found that it also sensitized these cells to IR, CPT, and cisplatin (Figures S1M and S1N), suggesting that the requirement for SUMO4 is not restricted to U2OS cells. We next disrupted the *SUMO4* locus using different gRNAs in independent U2OS clones (Figure S1O), creating stop-codon-inducing edits partway through *SUMO4*. Immunoblots of lysates indicated that the SUMO4 siRNA-sensitive band was absent from these clones (Figure 1N). No SUMO4-specific peptides were identified from clone 4.57, whereas the N-terminal peptide “PTEEVKTENNNHINLK” was identified in clone 1.11 (Figure S1C). Genes lacking the intron structure to regulate the decay of transcripts with premature stop codons often retain mutant mRNA expression,<sup>50</sup> and thus an expression of a severely truncated SUMO4 protein is expected. These clones are called U2OS-SUMO4<sup>T</sup> (truncated) hereafter. Both genomically targeted clones were sensitive to treatments with IR, CPT, and cisplatin (Figures 1O and S1P) and exhibited defects in 53BP1/RAD51 foci after IR exposure (Figure S1Q). Importantly, treating these cells with SUMO4 siRNA produced no additional defects in DSB signaling or survival (Figures S1Q and S1R), indicating *SUMO4* gene edits and SUMO4 siRNA disrupt the same cellular feature. As for siRNA treatment, the *SUMO4*-disrupted clones displayed normal levels of TAB2 protein (Figure S1S). The genetic, immunoblot, and functional data together indicate that the edited clones lack full SUMO4 activity.

SUMO4<sup>T</sup> cells retained a low level of IR-induced 53BP1 and RAD51 foci, which could be further reduced by RNF8/RNF168 or BRCA2 siRNA, respectively, suggesting that DSB repair signaling in these cells is substantially reduced, rather than absent (Figure S1T). To assess whether SUMO4 suppresses the chromosomal consequences of DNA damage, we analyzed

metaphase spreads and noted increased chromosomal breaks in IR-treated SUMO4<sup>T</sup> cells versus the parental U2OS (Figure 1O). Additionally, micronuclei, markers of fragmented or poorly segregated chromosomes, were increased in both IR-treated SUMO4<sup>T</sup> and siSUMO4 cells (Figures 1P and S1U). In summary, SUMO4 has little influence on MDC1 kinetics but promotes RNF168, 53BP1, and RAD51 foci accumulation. It promotes measures of homologous recombination (HR) and non-homologous end-joining (NHEJ) and is required for cellular resistance to genotoxins and the suppression of genomic instability.

### SUMO4 function is suppressed by its conjugation

To address whether conjugation proficiency relates to SUMO4 function, we made a series of siRNA-resistant SUMO4 mutants. These were in two categories: those designed to ensure conjugation incompetence and those altered to enable the mutant protein to be attached to target lysines through the SUMO conjugation pathway (conjugation proficient; Figure 2A). Conjugation-incompetent mutants carried a stop codon before the glycine residues essential for conjugation T91X (TX) or were mutant in those residues G92A/G93A (GA) and G92/G93A with V94X (GA/VX). As proline 90 is proposed to interfere with SENP-mediated exposure of the di-glycine motif, and to suppress SUMO4 maturation,<sup>8</sup> we generated a potentially conjugation-proficient mutant, SUMO4-P90Q (PQ), and also made an artificially matured variant bearing a stop codon after the glycine residues V94X (VX) (Figure 2A). As anticipated, only the SUMO4-PQ and SUMO4-VX mutants formed high molecular weight smears, indicating conjugation by the cellular SUMOylation machinery, whereas SUMO4-GA, SUMO4-TX, and SUMO4-GA/VX migrated as a monomer similar to SUMO4-WT (Figure 2B) suggesting that these are not conjugated. Further, conjugation-proficient mutants localized to the nucleus, whereas conjugation-deficient forms showed cytoplasmic and nuclear localization resembling the SUMO4-WT protein (Figure S2A).

We tested the mutants in complementation assays. Conjugation-incompetent variants (GA, TX, and GA/VX), but not proficient mutants (PQ and VX), restored 53BP1 and RAD51 foci to control/WT levels in SUMO4-deficient backgrounds (Figures 2C–2E, S2B, and S2C). Similarly, conjugation-incompetent (WT, TX, GA, and GA/VX), but not the conjugation-proficient

### Figure 2. Conjugation independent role of SUMO4 in DSB repair

(A) C-terminal tail of SUMO4. The di-glycine repeat is highlighted in green. The precursor tail removed by SENPs during Pro-SUMO maturation is gray. Stop codons are shown as X. Numbering relates to the SUMO4 sequence. The SUMO2 C terminus is shown for comparison. Expected conjugation proficiency is illustrated.

(B) SUMO4<sup>T</sup> cl1.11 cells transfected with FLAG-HA SUMO4 variants as illustrated, immunoblotted with HA antibody and GAPDH loading control.

(C) Representative images of cells treated with SUMO4 siRNA and expressing siRNA-resistant 6xHis-HA-SUMO4 variants before IR treatment (4 Gy), fixed 2 h later and immunostained for 53BP1 or RAD51. RAD51 foci are quantified in EdU + cells. Scale bar, 10 μm.

(D and E) Quantification of 53BP1 (D) or RAD51 (E) foci in SUMO4<sup>T</sup> cl1.11 cells expressing FLAG-HA SUMO4 variants before IR treatment (4 Gy). *N* = ~150 cells per condition from 3 experiments. Bars show mean ± SEM. Statistical analysis: one-way ANOVA.

(F) Colony assay of SUMO4<sup>T</sup> cl1.11 expressing FLAG-HA-SUMO4 proteins before irradiation (2 Gy). *N* = 3 from three independent experiments. Data are mean ± SEM. Statistical analysis: one-way ANOVA.

(G) Colony assay after SUMO4 siRNA treatment and expression of siRNA-resistant 6xHis-HA SUMO4 variants before exposure to 2 Gy IR. Data are mean ± SEM from three independent experiments. Statistical analysis: one-way ANOVA.

(H) HR and NHEJ reporter outcomes after co-transfection with SUMO4 siRNA and mRFP or His-HA-mRFP-SUMO4 variant expression. Data are mean ± SEM from three independent experiments. Statistical analysis: two-tailed *t* test.

(I) Micronuclei per cell from IR-treated (4 Gy, fixed 6 h later) in U2OS treated with SUMO4 siRNA and expressing siRNA-resistant 6xHis-HA-SUMO4 proteins. *N* = 5 independent experiments, 100 nuclei per condition. Data are mean ± SEM. Statistical analysis: one-way ANOVA.

See also Figure S2.



mutants (PQ and VX), restored cellular resistance to IR, CPT, cisplatin, and olaparib (Figures 2F, 2G, and S2D–S2I) and conjugation-proficient mutant, SUMO4-VX, could not restore GFP expression in either HR or NHEJ *SceI* reporter assays (Figure 2H). The suppression of micronuclei formation mirrored the SUMO4 mutants' ability to promote DSB signaling and survival (Figure 2I).

To address whether conjugation-proficient mutants are deleterious gain-of-function(s) variants, we examined their over-expression, finding expression of conjugation-proficient SUMO4 (PQ VX), but not WT protein, reduced cell survival after exposure to IR (Figure S2J), suggesting that SUMOylation is deleterious. We tested whether the expression of a conjugation-defective form of an alternative SUMO, SUMO2, complemented SUMO4<sup>T</sup> cells. Indeed, expression of SUMO2-GA (G92A/G93A) in SUMO4<sup>T</sup> cells improved 53BP1/RAD51 foci and cell survival after exposure to IR (Figures S2K–S2M), suggesting that either SUMO4 performs a role shared by free SUMO2 or that increased free SUMO2 suppresses the harmful consequences of absent SUMO4. Collectively, these results show that the conjugation of SUMO4 is incompatible with its function in DSB repair and indicate that non-physiological SUMO4 conjugates reduce survival after damage.

### SUMO4 requires its SIM-binding patch for DSB repair activity

SUMO4 shares several features with its SUMO2 ancestor, including the surface that proteins with SUMO-interacting motifs (SIMs) interact with (Figure 3A). We generated mutations analogous to the previously characterized SUMO2:SIM-interaction mutant,<sup>51</sup> SUMO4-Q31A/F32A/I34A (QFI-A), and found that while SUMO4-WT protein was pulled down by SIM-bearing peptides (derived from PIAS1 and SLX4 proteins), the mutant SUMO4-QFI-A protein was not (Figure S3A). SUMO4-WT and SUMO4-QFI-A showed similar subcellular localization (Figure S3B), but cells complemented with SUMO4-QFI-A were defective in 53BP1 and RAD51 foci formation, sensitive to DSB-inducing agents, and showed poor HR repair in integrated GFP gene-conversion assays (Figures 3F–3H and S3C–S3F). Micronuclei formation was also not suppressed by SUMO4-

QFI-A complementation (Figure 3I). These data implicate the SIM-SUMO4 interaction in the repair of DNA breaks.

### SUMO4 maintains SUMO1-3 homeostasis

We next assessed the impact of SUMO4 loss on cellular SUMOylation, noting that SUMO4<sup>T</sup> cells showed increased SUMO1 and SUMO2/3 conjugates (Figures 4A and S4A). Similarly, cells treated with SUMO4 siRNA showed elevated SUMO2/3 immunofluorescence intensity and elevated SUMO1 intensity after IR treatment (Figures 4B and 4C). Complementation with SUMO4-WT, but not SUMO4-QFI-A or conjugation-proficient mutants, suppressed these measures (Figures 4D, 4E, S4B, and S4C). We examined promyelocytic leukemia (PML) protein, PML nuclear bodies (PML-NBs), which are cellular features sensitive to altered SUMO conjugation,<sup>52,53</sup> and found increased numbers of PML-NBs here and in bodies containing the PML-NB component, Sp100, which could be restored to control levels by expression of SUMO4-WT but not SUMO4-QFI-A (Figures S4D–S4G).

We considered whether the increased cellular SUMOylation might influence DSB repair proficiency of SUMO4-deficient cells. We tested short-term treatment with the SUMO E1 inhibitor ML-792,<sup>54</sup> finding, remarkably, that ML-792 addition improved 53BP1 and RAD51 foci accrual and cellular resistance to IR (Figures 4F–4J). We then partially depleted the SUMO E2, UBC9, which also improved IR resistance and 53BP1 and RAD51 foci in SUMO4-deficient cells (Figures 4K–4N). Analysis of cells treated with siRNAs targeting PIAS1–4 SUMO E3 ligases determined that PIAS1 siRNA treatment improved 53BP1 and RAD51 foci numbers and resistance to IR, CPT, and olaparib in SUMO4<sup>T</sup> cells (Figures S4H–S4M). These data suggest that hyper-PIAS1-dependent SUMOylation underlies defective DSB signaling in the absence of SUMO4.

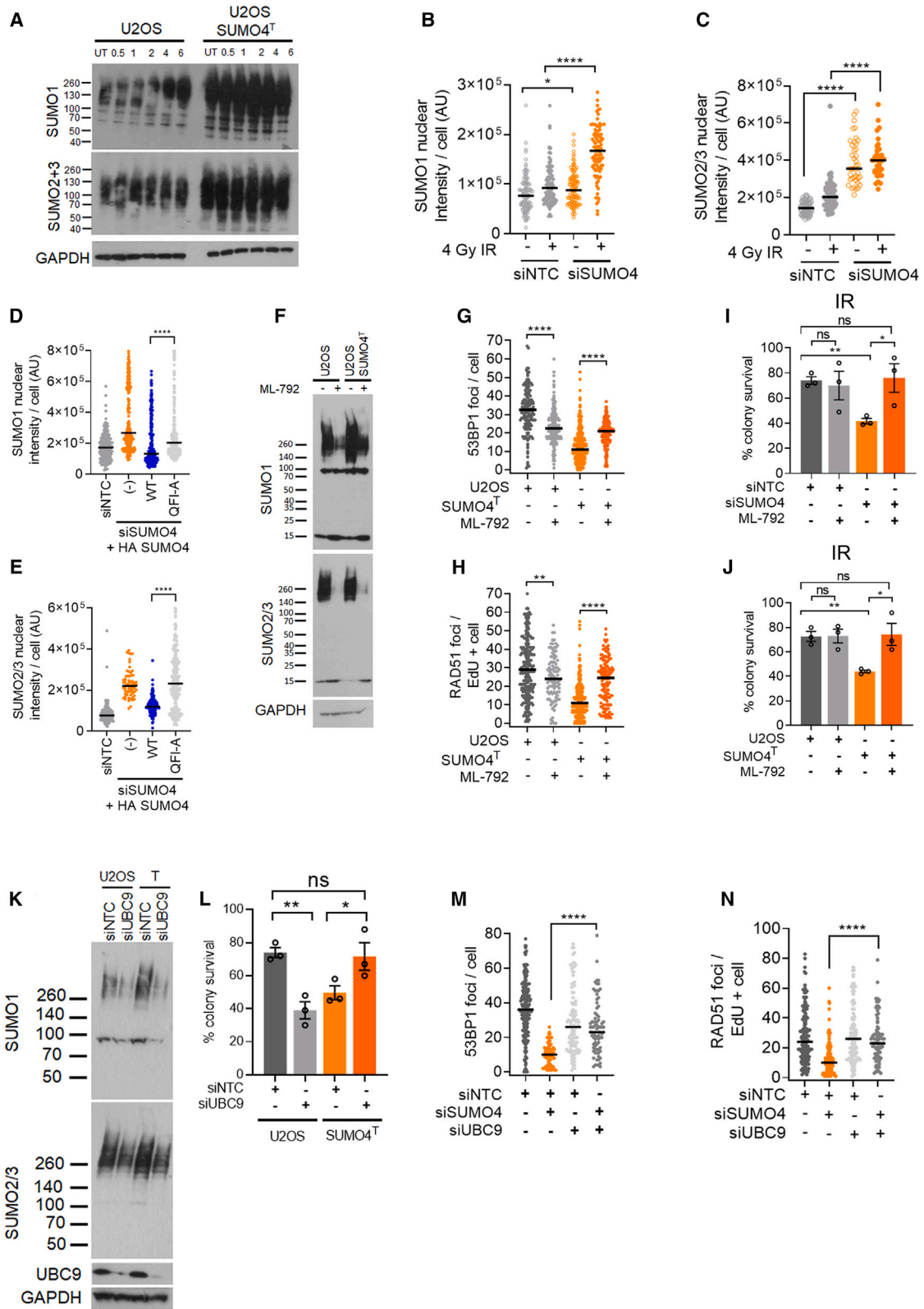
### SUMO4 promotes SENP1 protease activity

To determine whether increased SUMO conjugates are driven by altered turnover, we prepared cellular extracts without the cysteine protease inhibitors that are usually included to suppress the protease-mediated cleavage of Ub/Ubl conjugates. SUMO4<sup>T</sup> cells showed a slower rate of reduction of high molecular weight SUMO conjugates than parental cells, which could be restored

### Figure 3. SUMO4 requires its SIM-binding groove to promote DSB repair activity

- (A) Alignment of human SUMO1 (P63165), SUMO2 (P61956), SUMO3 (P55854), and SUMO4 (Q6EEV6). The SIM-binding groove is highlighted.
- (B) Immunoblot of SUMO4<sup>T</sup> cl1.11 cells expressing FLAG-HA-SUMO4-WT or FLAG-HA-SUMO4-QFI-A mutant, probed with antibodies to HA and GAPDH.
- (C) Representative images of 53BP1 and RAD51 foci in cells treated with siSUMO4 and expressing siRNA-resistant 6xHis-HA-SUMO4 variants before IR (4 Gy), fixed 2 h later. EdU marks S phase cells. Scale bars, 10  $\mu$ m.
- (D) 53BP1 foci in parental or SUMO4<sup>T</sup> cl1.11 cells complemented with FLAG-HA-SUMO4-WT or FLAG-HA-SUMO4-QFI-A before IR (4 Gy), fixed 2 h later. >150 cells per condition from 3 experimental repeats. Bar shows mean  $\pm$  SEM. Statistical analysis: two-tailed t test.
- (E) RAD51 foci scored in EdU-positive cells as in (D).
- (F) Colony assay of SUMO4<sup>T</sup> cl1.11 cells expressing FLAG-HA-SUMO4-WT or FLAG-HA-SUMO4-QFI-A and treated with IR (2 Gy). Data are mean  $\pm$  SEM from three independent experiments. Statistical analysis: two-tailed t test.
- (G) Colony assay of cells treated with (NTC) siRNA or siRNA to SUMO4 and expressing 6xHis-HA-SUMO4 proteins before IR (2 Gy) treatment. Data are mean  $\pm$  SEM from three independent experiments. Statistical analysis: two-tailed t test.
- (H) HR reporter outcomes after siRNA SUMO4 and expression of 6xHis-HA-mRFP-SUMO4 variants are shown relative to those treated with NTC. *N* = 3 experimental repeats, each performed in triplicate. Data are mean  $\pm$  SEM. Statistical analysis: two-tailed t test.
- (I) Micronuclei per cell from IR-treated (4 Gy, fixed 6 h later) in 6xHis-HA-SUMO4 complemented siSUMO4-treated cells and SUMO4<sup>T</sup> cl1.11 cells. *N* = 5 independent experiments with  $\sim$ 100 nuclei counted per experiment. Data are mean  $\pm$  SEM. Statistical analysis: two-tailed t test.

See also Figure S3.



(legend on next page)

by the expression of exogenous SUMO4-WT (Figures 5A–5D), suggesting a slower rate of SUMO1–3 substrate deconjugation in SUMO4<sup>T</sup> extracts.

To test whether SUMO4 influences particular SUMO proteases, we incubated cell lysates with HA-SUMO1- or HA-SUMO2-Vinyl sulfone (SUMO1-VS and SUMO2-VS, respectively). These are active site-directed irreversible inhibitors of SENPs that can act as a proxy for the catalytic activity or catalytic cysteine availability.<sup>55</sup> We measured the labeling of SENP1, SENP3, and SENP6 SUMO proteases. Of these, only SENP1 showed reduced labeling in SUMO4<sup>T</sup> cell lysates (Figures 5E, 5F, and S5A–S5D). We examined the impact of SENP1 depletion on SUMO2/3 deconjugation, noting a slowing of SUMO2/3 conjugate reduction (Figure S5E). Moreover, the expression of SUMO4-WT, but not SUMO4-QFI-A, improved SUMO1-VS labeling of SENP1 in SUMO4-deficient cells (Figure 5G), indicating that SUMO4-WT enhances accessibility to the SENP1 catalytic site. These data imply that SUMO4 may positively regulate SENP1 catalytic function.

We therefore examined SENP1 protease activity *in vitro*, incubating the SENP1 catalytic domain (SENP1c) with recombinant SUMO4-WT and QFI-A (rSUMO4) proteins and assessing three SENP1 protease activities: proSUMO3 maturation, diSUMO2 cleavage, and deconjugation of SUMO1 from the minimal SUMOylated fragment of RanGAP1 (amino acids 398–587). In each case, incubation of the SENP1c with rSUMO4-WT increased deconjugation activity (Figures 5H–5J). rSUMO4-QFI-A was slightly less efficient than rSUMO4-WT at promoting SENP1c's proSUMO3 maturation and diSUMO2 cleavage activity but was less able to promote RANGAP-1 deSUMOylation (Figures 5H–5J). The stimulation of protease activity was specific to rSUMO4, as neither rSUMO1 nor rSUMO2 (WT or QFI-A) increased SENP1c activity against RANGAP1-SUMO1 (Figure S5F). We next made and tested the C-terminal mutants of rSUMO4 (T91X and V94X) and also tested proSUMO2 bearing proline at codon 90 (i.e., making C-terminal SUMO2 more SUMO4-like). We found rSUMO4 (T91X and V94X) enhanced SENP1c deSUMOylation of RANGAP1-SUMO1, whereas the

mutant SUMO2 did not (Figure S5G), suggesting the C-terminal “P..VY” residues of SUMO4 are not responsible for promoting SENP1 catalytic activity *in vitro* and indicating that conjugation ability, in the context of free SUMO, does not suppress SUMO4's ability to promote SENP1 activity. With the addition of chemical crosslinkers, we could detect an association between rSUMO4-WT and SENP1c and a weak association between rSUMO4-WT and rSUMO2 (Figure S5H). Incubation of rSUMO4-WT and SENP1c in the presence of excess SLX4-SIM peptide, but not a peptide in which the hydrophobic residues of the SIM were mutated, reduced the production of the crosslinking rSUMO4-WT complex (Figure S5I), implying that a SIM interface contributes to the formation or stability of the complex.

A role for SENP1 catalytic activity in DSB repair has not been defined. We complemented SENP1 siRNA-treated U2OS with siRNA-resistant forms of SENP1, either SENP1-WT or SENP1-C603A (catalytic active site mutant<sup>56</sup>). SENP1-WT, but not SENP1-C603A, restored  $\gamma$ H2AX, 53BP1, and RAD51 foci numbers to control levels; promoted the survival of U2OS treated with IR, CPT, cisplatin, or olaparib; and suppressed micronuclei formation (Figures S5J–S5O), suggesting that SENP1's catalytic function promotes DSB repair. We assessed the relationship of SENP1 with SUMO4 by performing siRNA co-depletions. In measures of DSB signaling to generate RAD51 and 53BP1 foci as well as suppression of micronuclei and survival in response to IR, CPT, cisplatin or olaparib, we found that combined SUMO4/SENP1 siRNA treatments were no more deleterious than the impact of each siRNA alone (Figures 5K–5N and S5P–S5R). These data are consistent with the notion that SUMO4 promotes SENP1 catalytic function during DSB repair.

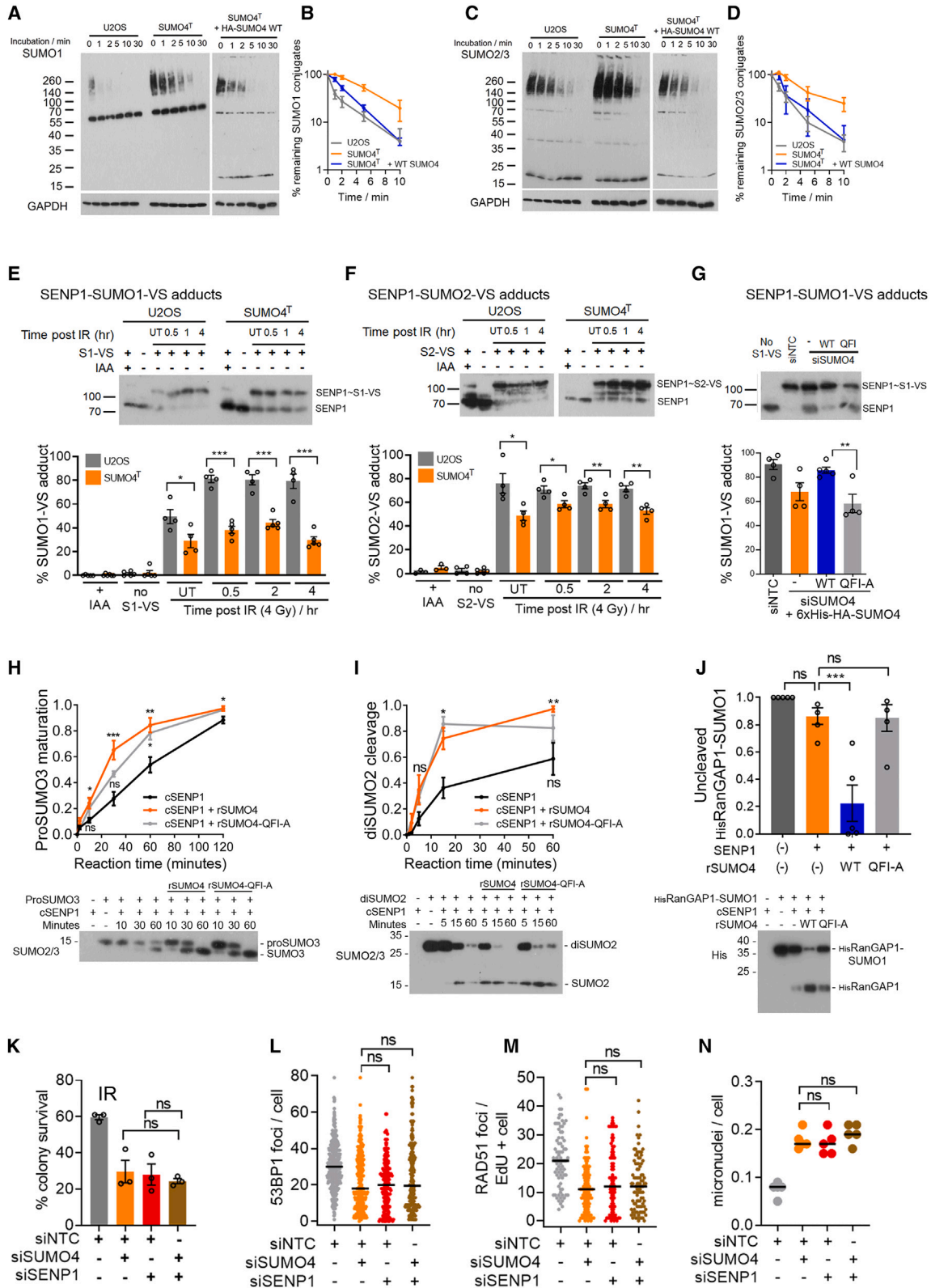
### The SUMO-dependent accumulation of RAP80 at DSBs is regulated by SUMO4-SENP1

Our findings indicate that SUMO4 deficiency disrupts DSB signaling through increasing SUMO conjugates. We hypothesized that a component of the DSB response capable of recognizing SUMO might direct the disruption. The BRCA1-A complex

#### Figure 4. SUMO4 maintains SUMO1–3 homeostasis

- (A) Parental of SUMO4<sup>T</sup> cl1.11 treated with 4 Gy IR, lysed at indicated time points, and immunoblotted for SUMO1, SUMO2/3, and GAPDH loading control.  
 (B and C) Immunofluorescence intensity of SUMO1 (B) and SUMO2/3 (C) after treatment with control siRNA (siNTC) or SUMO4 siRNA (siSUMO4) and 4 Gy IR, followed (after 2 h) by pre-extraction, fixing, and immunostaining with the relevant antibodies. Fluorescence intensity per cell in arbitrary units (a.u.) from ~100 cells per condition. Bars show mean  $\pm$  SEM. Statistical analysis: two-tailed t test.  
 (D and E) Quantification of indirect immunofluorescence intensity assessed as in (B) and (C), of SUMO1 (D) or SUMO2/3 (E), following SUMO4 siRNA and 6 $\times$ His-HA-SUMO4 variant expression.  $N = \sim 150$  cells per condition from a total of three experiments. Bars show mean  $\pm$  SEM. Statistical analysis: two-tailed t test.  
 (F) Parental and SUMO4<sup>T</sup> cl1.11 cells treated with 1  $\mu$ M ML-792 (+) or DMSO (–) and immunoblotted with antibodies to SUMO1, SUMO2/3, and GAPDH.  
 (G and H) Quantification of 53BP1 foci (G) and RAD51 foci (H) in SUMO4<sup>T</sup> cl1.11 cells treated with 1  $\mu$ M ML-792 or DMSO for 1 h before irradiation (4 Gy), fixed 2 h later, and immunostained for the relevant proteins.  $n = \sim 150$  cells per condition from 3 experiments. Bars show mean  $\pm$  SEM. Statistical analysis: two-tailed t test.  
 (I) Colony assay of U2OS treated with siNTC or siSUMO4 and either 1  $\mu$ M ML-792 or DMSO for 1 h before irradiation (2 Gy). Data are mean  $\pm$  SEM.  $N = 4$  independent experiments. Statistical analysis: two-tailed t test.  
 (J) Colony assay of parental and SUMO4<sup>T</sup> cl1.11 cells treated with 1  $\mu$ M ML-792 or DMSO for 1 h before irradiation (2 Gy),  $n = 4$ . Data are mean  $\pm$  SEM from three independent experiments. Statistical analysis: two-tailed t test.  
 (K) Immunoblot of parental U2OS or SUMO4<sup>T</sup> cl1.11 cell lysates (T) after siNTC or UBC9 siRNA treatment using primary antibodies shown.  
 (L) Colony assay of parental U2OS or SUMO4<sup>T</sup> cl1.11 cells treated with UBC9 siRNA prior to IR (2 Gy).  $N = 3$  independent experiments. Data are mean  $\pm$  SEM. Statistical analysis: one-way ANOVA.  
 (M and N) 53BP1 foci (M) and RAD51 foci (N) in cells treated with siNTC or siSUMO4, with or without UBC9 siRNA (siUBC9) before irradiation (4 Gy), fixed after 2 h.  $N \geq 75$  cells per condition from a total of three experiments. RAD51 foci were scored in EdU + cells. Bars show mean  $\pm$  SEM from >80 nuclei per analysis. Statistical analysis: two-tailed t test.

See also Figure S4.



(legend on next page)

component RAP80 (UIMC1/ubiquitin-interacting motif containing 1) contains tandem SIM-ubiquitin interaction motifs (UIMs) that interact with SUMO2/3 and K63-ubiquitin chains.<sup>43,44,57</sup> To determine whether RAP80 is affected by SUMO4 disruption, we assessed RAP80 foci in irradiated U2OS cells treated with siRNAs to SUMO1–4. In agreement with prior findings<sup>43,44</sup> and the dependence of upstream ubiquitin signaling on SUMO1–3 (Figure 1), depletion of SUMO1 or SUMO2/3 reduced RAP80 foci (Figure 6A). Conversely, SUMO4-siRNA caused a hyper-accumulation of RAP80 foci, which could be reversed by complementation with SUMO4-WT but not SUMO4-QFI-A (Figure 6B). Similarly, siRNA targeting SENP1, but not siRNAs targeting other SENP proteins, resulted in increased RAP80 foci after IR exposure (Figure S6A). Further, the increased RAP80 foci induced by siRNA SENP1 treatment could be suppressed by SENP1-WT complementation but not by SENP1-C603A (Figures 6C and 6D), whereas over-expression of SENP1 reduced IR-induced RAP80 foci numbers in a catalytic-dependent manner (Figure S6B). Co-depletion of SENP1 and SUMO4 did not increase RAP80 foci numbers more than either depletion alone (Figure 6E), consistent with an epistatic relationship between these proteins in promoting DSB repair.

We assessed the dependence of the accumulations of RAP80 in SUMO4<sup>T</sup> cells and, as expected, found that they required both upstream K63-Ub signaling components and components of the SUMO conjugation system, including PIAS1 (Figures S6C–S6E). Further, we tested mutant RAP80, disrupted in its SUMO-interaction motif, F40A/V41A/I42A (hereafter RAP80<sup>SIM</sup>, Hu et al.<sup>43</sup>) and found that, unlike RAP80<sup>WT</sup>, the SIM mutant did not show increased accumulation in irradiated SUMO4-depleted cells (Figure S6F). Thus, the increased formation of RAP80 foci, observed following SUMO4 loss, requires active SUMOylation and SUMO-SIM interactions.

We used two approaches to determine whether the increased accumulation of RAP80 contributes to the DSB repair defect in

SUMO4-deficient cells. First, we tested the over-expression of RAP80<sup>SIM</sup> because the SIM residues of RAP80 are required to recruit RAP80. Remarkably, RAP80<sup>SIM</sup> over-expression in SUMO4-deficient cells improved 53BP1 and RAD51 foci accrual and cellular resistance to IR, CPT, and olaparib (Figures 6F–6I and S6G). Second, we tested the impact of SUMO2<sup>K21R</sup> expression. Biochemical studies using defined lysine SUMO-ubiquitin linkages suggest K63-ubiquitin dimers conjugated to lysine 21 of SUMO2 are preferentially recognized by the SIM-UIM module of RAP80.<sup>58</sup> We found that RAP80 foci numbers in irradiated SUMO4<sup>T</sup> cells were suppressed to parental levels when SUMO2<sup>K21R</sup> mutant—but not SUMO2<sup>K11R</sup> mutant—was expressed (Figures 6J–6L), consistent with a requirement for SUMO2<sup>K21</sup> in RAP80 recruitment. Further, SUMO2<sup>K21R</sup> expression increased 53BP1 and RAD51 foci after IR and increased resistance to IR, CPT, and olaparib of SUMO4-deficient cells (Figures 6M–6O, S6H, and S6I). Collectively, these data suggest that increased SUMO-dependent accumulation of RAP80 contributes to the DSB repair defect in SUMO4-deficient cells.

The BRCA1-A complex comprises RAP80, Abraxas/CCDC98, BRCC36, BRCC45, MERIT4, and a proportion of cellular BRCA1:BARD1 heterodimer.<sup>59</sup> The deubiquitinating enzyme, BRCC36, cleaves K63-Ub chains, while phosphorylated Abraxas interacts with the C-terminal BRCT repeats of BRCA1 and recruits the BRCA1-BARD1 heterodimer.<sup>60–66</sup> To test whether these activities contribute to defective DSB repair in SUMO4-deficient cells, we over-expressed a catalytic mutant of BRCC36, H124Q/H126Q<sup>67</sup> (BRCC36-HQ) and a mutant of Abraxas in which the target residues of phosphorylation were substituted, S404A/S406A<sup>68</sup> (Abraxas-SA). Expression of BRCC36-HQ, but not Abraxas-SA, restored IR-induced 53BP1 and RAD51 foci in irradiated SUMO4-deficient cells (Figures 6P and 6Q). Expression of BRCC36-HQ also improved the resistance of SUMO4-deficient cells to IR, CPT, and olaparib (Figures 6R, S6J, and S6K), and the Abraxas-SA mutant

### Figure 5. SUMO4 modulates SENP1 SUMO protease activity

(A–D) Immunoblot of SUMO1 (A) or SUMO2/3 (C) in U2OS, SUMO4<sup>T</sup> cl. 11, and SUMO4<sup>T</sup> cl. 11 expressing FLAG-HA-SUMO4-WT. At the 0 time point, cells were lysed in cysteine-protease-inhibitor-containing buffer; for all other time points, they were lysed without. Graph shows densitometry of the >70 kDa SUMO signal relative to the 0 time point. Data are mean ± SEM. Graphs show SUMO1 (B) or SUMO2/3 (D) proteins. Each graph; *n* = 3 experiments.

(E and F) At time points after 4 Gy IR, lysates were incubated with HA-SUMO1-vinyl sulfone (S1-VS) (E) and HA-SUMO2-vinyl sulfone (S2-VS) (F), denatured, and immunoblotted with SENP1 antibody. The relative amount of upper band (SUMO-VS labeled SENP1) versus unlabeled SENP1 (lower band) was used to calculate % SENP1-SUMO-VS adduct formation. IAA, incubation with cysteine protease inhibitor; no S1-VSHA, SUMO1-vinyl-sulfone was omitted. Each graph; *N* = 4 experiments. Data are mean ± SEM. Statistical analysis: two-tailed t test.

(G) SENP1 HA-SUMO1-vinyl sulfone labeling of cells treated with siNTC or siSUMO4 siRNA and expressing 6 × His-HA-SUMO4-WT or 6 × His-HA-SUMO4-QFI-A. *N* = 4 experiments. Data are mean ± SEM. Statistical analysis: two-tailed t test.

(H) Generation of mature SUMO3 from pro-SUMO3 by the SENP1 catalytic domain (SENP1c) in the presence of SUMO4 variants. SENP1c was incubated with recombinant SUMO4 (rSUMO4) before the addition of pro-SUMO3 and incubated for times shown before immunoblotting for SUMO2/3. The graph shows the proportion of the lower SUMO3, cleaved product, of total SUMO3. *N* = 4 experiments. Data are mean ± SEM. Statistical analysis: one-way ANOVA.

(I) Cleavage of diSUMO2 by SENP1c in the presence of SUMO4 variants. 25 nM. Monomeric SUMO2 as a proportion of total SUMO2 is shown in the graph. *N* = 7 experiments. Data are mean ± SEM. Statistical analysis: one-way ANOVA.

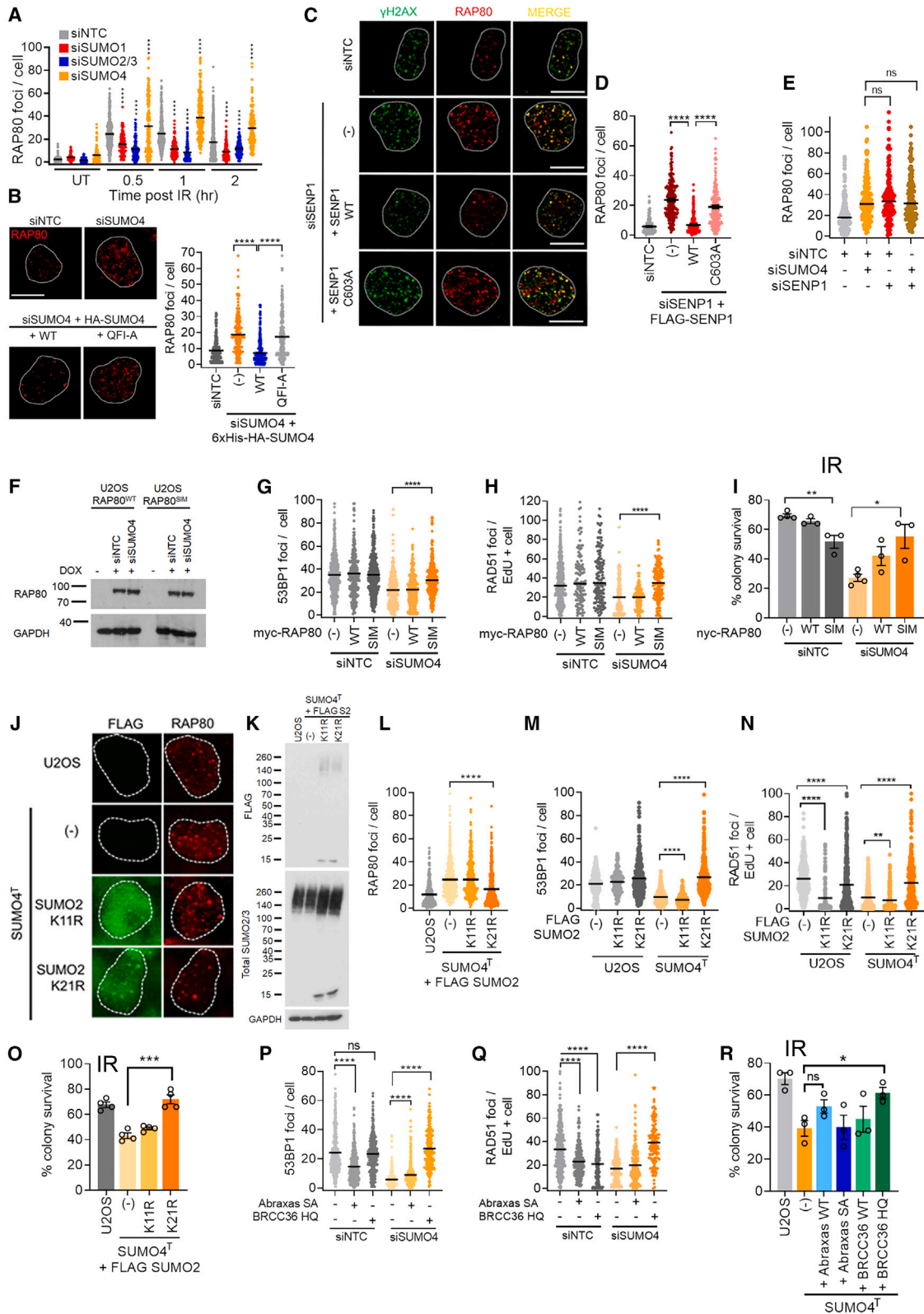
(J) DeSUMO-1ylation of RanGAP1-SUMO1 by SENP1c in the presence of SUMO4 variants. The amount of HisRanGAP1-SUMO1 (top band) relative to samples without SENP1c is shown. *N* = 5 experiments. Data are mean ± SEM. Statistical analysis: two-tailed t test.

(K) Colony assay of U2OS treated with non-targeting siNTC, siRNA to SENP1, SUMO4, or both before irradiation (2 Gy). *N* = 3. Data are mean ± SEM from three independent experiments. Statistical analysis: two-tailed t test.

(L and M) 53BP1 (L) or RAD51 (M) foci in U2OS treated with siNTC, siRNA to SENP1, SUMO4, or both before irradiation (2 Gy), fixed 2 h later and immunostained. *N* = ~150 cells per condition from 3 experimental repeats. Bars show mean ± SEM. Statistical analysis: two-tailed t test.

(N) Micronuclei per cell after irradiation (4 Gy). *N* = 4 experiments, 100 nuclei per condition per experiment. Bars are mean ± SEM. Statistical analysis: two-tailed t test.

See also Figure S5.



(legend on next page)

improved resistance to CPT and Olaparib but not IR (Figures 6R, S6K, and S6L). These data indicate that suppressing aspects of the BRCA1-A complex activity can overcome the deleterious impact of SUMO4 loss.

## DISCUSSION

Our analysis confirms distinct roles for SUMO1 and SUMO2/3 in signaling the DNA DSB response<sup>21,33</sup> and demonstrates an unexpected role for SUMO4. The SUMO1-3 system is well-characterized,<sup>69</sup> but the indication that SUMO4 is unconjugated, combined with a lack of specific SUMO4 detection reagents,<sup>2</sup> and few unique peptide sequences in MS analysis have led to SUMO4 being overlooked.

Here, we demonstrate that SUMO4, but not SUMO1 or SUMO2, acts to stimulate SENP1 catalytic activity *in vitro* and that SUMO4 promotes SENP1 catalytic activity in cells. The requirement for the SUMO4 SIM-interaction face in promoting SENP1 protease activity against a model-substrate *in vitro* and in supporting DSB signaling in cells is intriguing. Possible mechanisms of SUMO4 action include suppression of product inhibition to which SENP1 is subject<sup>56</sup> and allosteric activation; we observed that excessive SIM availability suppresses the formation of the SUMO4:SENP1 complex *in vitro*, but whether SUMO4 activation occurs through SENP1 or through the substrate/product SUMOs awaits further biochemical and structural assessment.

In acting as an unconjugated ubiquitin-like modifier, SUMO4 bears some similarity to UBL5 (ubiquitin-like protein 5), which is not conjugated due to a di-tyrosine motif in place of the di-

glycine. UBL5 instead signals through non-covalent interactions with partner proteins.<sup>70</sup>

We find a crucial role for SUMO4:SENP1 in restricting the SUMO signaling responsible for RAP80 recruitment and, consequently, for promoting DSB repair. RAP80 is part of the BRCA1-A complex, and expressing mutant components of the complex relieves the poor DNA damage signaling and genotoxin sensitivities of SUMO4-deficient cells. These findings imply that excessive or prolonged BRCA1-A complex activity is deleterious, consistent with its reported ability to restrict ubiquitin signaling and DNA resection.<sup>60-62,67,71,72</sup> Optimal accumulation of RAP80 to DSBs depends on ubiquitin, SUMO, and TRAIIP binding,<sup>73,74</sup> and the recruiting substrate(s) are presumed to be modified histones or modified, recruited repair proteins.<sup>74-76</sup> It is feasible that SENP1 locally deSUMOylates concentrated, modified proteins in a manner similar to the activity of SENP6, which deSUMOylates multiple centromeric proteins to support mitosis.<sup>77,78</sup>

Our findings delineate the SUMO E3 ligase:SUMO protease pair of PIAS1-SENP1, showing they regulate the SUMO conjugates recognized by RAP80. Our data show that this pair are distinct from the previous E3 ligase:SUMO protease pair of PIAS4-SENP2, responsible for MDC1-SUMOylation regulation in G1 cells.<sup>28-31,33</sup> Thus, cells initiate at least two distinct waves/sprays of SUMOylation/deSUMOylation in the DSB response. The degree to which other SUMO/deSUMOylation events are part of these waves or are distinct remains to be seen.

We note that the impact of SUMO4 loss on SUMO-conjugate turnover is not restricted to DNA-damage-treated cells but also occurs in untreated conditions (e.g., Figure 4A). We predict

### Figure 6. The accumulation of RAP80 is regulated by SUMO4-SENP1

- (A) RAP80 foci after indicated siRNA treatments and irradiation (4 Gy), fixed at the indicated times and immunostained.  $N > 100$  cells per condition from three experiments. Bars are mean  $\pm$  SEM. Statistical analysis: two-tailed t test between siNTC and siSUMO for each time point.
- (B) RAP80 foci in cells treated with SUMO4 siRNA, expressing 6 $\times$ His-HA-SUMO4-WT or 6 $\times$ His-HA-SUMO4-QF1-A irradiated (4 Gy), and fixed 2 h later. Images, left, scale bar, 10  $\mu$ m.  $N \sim 150$  cells per condition from three experiments. Bars are mean  $\pm$  SEM. Statistical analysis: two-tailed t test.
- (C and D) RAP80 foci in U2OS treated with siNTC, or SENP1 siRNA (siSENP1), expressing siRNA-resistant FLAG-SENP1 variants, irradiated (4 Gy) and fixed 2 h later. (C) Shows representative images of RAP80 and  $\gamma$ H2AX, scale bars, 10  $\mu$ m (D). RAP80 foci per cell from  $\sim 150$  cells per condition from three experiments. Bars are mean  $\pm$  SEM. Statistical analysis: two-tailed t test.
- (E) RAP80 foci after treatment with the siRNAs shown and irradiation (2 Gy).  $N = 150$  cells per condition from a total of three independent experiments. Bars are mean  $\pm$  SEM. Statistical analysis: two-tailed t test.
- (F) Immunoblot of doxycycline-inducible Myc-RAP80<sup>WT</sup> and Myc-RAP80<sup>SIM</sup> (SUMO-interacting motif mutant) treated (+) or not (-) with doxycycline in siNTC or siSUMO4 treated cells (48 h). The blots were probed for Myc and GAPDH.
- (G and H) Assessment of 53BP1 (G) and RAD51 foci (H) after siNTC or siSUMO4 siRNA- treatment, following induction of RAP80<sup>WT</sup> or Myc-RAP80<sup>SIM</sup> (WT, SIM) or not (-) and irradiation (2 Gy).  $N > 100$  cells per condition for a total of three experiments. Bars are mean  $\pm$  SEM. Statistical analysis: two-tailed t test.
- (I) Colony assay of cells treated with NTC or SUMO4 siRNAs and expressing Myc-RAP80<sup>WT</sup> or Myc-RAP80<sup>SIM</sup> for 48 h, and treated (WT, SIM) or not (-) and irradiated (2 Gy).  $N = 3$  independent experiments. Data are mean  $\pm$  SEM. Statistical analysis: two-tailed t test.
- (J) Images of RAP80 foci in SUMO4<sup>T</sup> cl1.11 U2OS expressing doxycycline-inducible FLAG-SUMO2<sup>K11R</sup> or SUMO2<sup>K21R</sup>, irradiated (4 Gy), fixed 2 h later.
- (K) Immunoblot of FLAG-SUMO2 mutants and SUMO2/3 in SUMO4<sup>T</sup> cl1.11 cells.
- (L) RAP80 foci in parental U2OS or SUMO4<sup>T</sup> cl1.11 expressing FLAG-SUMO2<sup>K11R</sup> or SUMO2<sup>K21R</sup> before 4 Gy irradiation.  $N > 100$  cells per condition. Bars are mean  $\pm$  SEM. Statistical analysis: two-tailed t test.
- (M and N) 53BP1 foci (M) and RAD51 foci (N) in parental or SUMO4<sup>T</sup> cl1.11 cells expressing FLAG-SUMO2<sup>K11R</sup> or SUMO2<sup>K21R</sup> and 4 Gy irradiation.  $N > 100$  per condition for a total of three experiments. Bars are mean  $\pm$  SEM. Statistical analysis: two-tailed t test.
- (O) Colony assay following exposure to 2 Gy IR in parental U2OS or SUMO4<sup>T</sup> cl1.11 cells expressing FLAG-SUMO2<sup>K11R</sup> or SUMO2<sup>K21R</sup>  $N = 4$ . Data are mean  $\pm$  SEM. Statistical analysis: two-tailed t test.
- (P and Q) 53BP1 foci (P) and RAD51 foci (Q) in parental and SUMO4<sup>T</sup> cl1.11 cells treated with NTC or SUMO4 siRNAs expressing Abraxas (SA phosphorylation/BRCA1 interaction mutant) or BRCC36 (HQ catalytic inactive mutant) expression, exposed to IR (4 Gy), fixed 2 h later.  $N > 100$  per condition for a total of three experiments. Bars are mean  $\pm$  SEM. Statistical analysis: two-tailed t test.
- (R) Colony assay of SUMO4<sup>T</sup> cl1.11 cells expressing Abraxas or BRCC36 variants and irradiated (2 Gy).  $N = 3$ . Data shows mean  $\pm$  SEM. Statistical analysis: two-tailed t test.

See also Figure S6.

that SUMO4 regulation of SENP1 activity is relevant to SENP1-mediated SUMO-conjugate homeostasis beyond DNA damage and repair. Dysregulation of the SUMO machinery contributes to tumorigenesis and drug resistance of various cancers, and both SUMO conjugation and deconjugation enzymes are considered drug targets.<sup>54,79,80</sup> The discovery of SUMO4 as a component promoting deSUMOylation brings potential new means to target the SUMO pathway.

### Limitations of the study

This work represents evidence that SUMO4 has a functional role in DSB repair. One limitation is that we have tested its over-expression in the context of depleted and genetic knockout cells. Some effects observed reveal the non-physiological impacts of manipulating the SUMO system. For example, over-expression of a non-conjugatable form of SUMO2, SUMO2-GA, can suppress the requirement for SUMO4. As SUMO2 cannot activate SENP1 *in vitro*, we speculate that excessive free SUMO2 may relieve some of the deleterious impacts of increased SUMO conjugates, perhaps by competing for the SIM-binding interface of RAP80. Similarly, although over-expression of WT-SUMO4 has no impact on repair outcomes, over-expression of conjugation-proficient SUMO4 is deleterious to DNA repair. We speculate that, due to differing charges of several of its surfaces, SUMO4 incorporation into conjugates may suppress vital protein:protein interactions. We have shown endogenous SUMO4 protein and note that its expression levels are below that of free SUMO2/3. Previous peptide identification has found that peptides unique to SUMO4 in human primary tissue and cell lines are at levels far below those for other SUMO proteins.<sup>81</sup> MS evidence is challenging due to the low abundance of SUMO4, combined with the challenges in quantifying peptide abundances from in-gel digests. We reported medium-confidence SUMO-4 N-terminal peptides U2OS in the cells, but quantification should be taken with extreme caution. We anticipate SUMO4 is present at levels below that of SENP1. The precise mechanism by which SUMO4 stimulates SENP1 protease function, and the impact SUMO4 has on diverse cellular SENP1 substrates, remains unclear and a topic for future work.

### RESOURCE AVAILABILITY

#### Lead contact

Further information and requests for resources and reagents should be directed to the lead contact, Joanna. R. Morris, [j.morris.3@bham.ac.uk](mailto:j.morris.3@bham.ac.uk).

#### Materials availability

All reagents and materials are listed in the [key resources table](#). All materials generated in this study are available from the [lead contact](#) upon request.

#### Data and code availability

- Liquid chromatography-tandem mass spectrometry (LC-MS/MS) data have been deposited in the ProteomeXchange with the identifier PXD054695 and are available as of the date of publication. All unprocessed data image files have been deposited at the Mendeley database with the DOI given in the [key resources table](#) and are available as of the date of publication.
- This paper does not report original code.
- Any additional information required to reanalyze the data reported in this paper is available from the [lead contact](#) upon request.

### ACKNOWLEDGMENTS

Grant funding: Wellcome Trust 206343/Z/17/Z (A.J.G., M.J.W.M., and A.K.W.), University of Birmingham (A.J.L. and R.M.D.), BBSRC/MIBTP BB/T00746X/1 (Y.A.), CRUK C8820/A19062 and C8820/A28283 (R.M.D., K.S., G.E.R., M.J.W.M., and H.M.), Royal Society RG\R1\241093 (J.S.B.), and University of Leeds (A.J.G.). The U2OS Myc-RNF168 cells were generated by Anoop Singh-Chauhan. We thank the Microscopy and Imaging Services at Birmingham University (MISBU) in the Tech Hub facility for microscope support and maintenance. We thank Jeremy Stark (City of Hope, Duarte, USA) for U2OS DR-GFP and NHEJ-EJ5 cells. UbcH9 (human UBC9) plasmid was a gift from Peter Howley (Addgene plasmid # 8651). pET23a-His-hRanGAP1tail, pET28a-His-hAos1, and pET28b-hUba2-His were gifts from Frauke Melchior (Addgene plasmid # 53139, # 53135, and # 53117). We thank the Advanced Mass Spectrometry Facility at the University of Birmingham for assistance with the mass spectrometry measurements. We thank Ron Hay for helpful discussions.

### AUTHOR CONTRIBUTIONS

A.J.G. designed the study and undertook blots, cell work, imaging, and analysis; A.J.L. generated purified recombinant proteins and performed *in vitro* assays and western blots; K.S. conducted metaphase spreads; R.M.D. performed Scel reporter assays; Y.A. carried out colony assays; H.M. validated siRNA; A.K.W. analyzed the cell-cycle; G.E.R. optimized native SUMO4 immunoprecipitations for LC-MS/MS analysis; M.J.W.M. performed LysC digestion, LC-MS/MS, and protein crosslinking; J.S.B. performed western blots; A.J.G. supervised J.S.B.; A.C.L. supervised M.J.W.M. and MS data analysis; and J.R.M. oversaw the study. A.J.G. and J.R.M. co-wrote the paper. All authors have commented on and edited the manuscript.

### DECLARATION OF INTERESTS

The authors declare no competing interests.

### STAR★METHODS

Detailed methods are provided in the online version of this paper and include the following:

- [KEY RESOURCES TABLE](#)
- [EXPERIMENTAL MODEL AND STUDY PARTICIPANT DETAILS](#)
  - Mammalian cell culture, stable cell lines, and SUMO4<sup>T</sup> cells
- [METHOD DETAILS](#)
  - Transfections
  - Cell cycle analysis
  - Non-denaturing SUMO immunoprecipitation
  - Proteomics analysis
  - Immunofluorescence
  - Modified lysis and SDS-PAGE (for SUMO4 separation)
  - Cell survival colony assays
  - DNA repair reporter assays
  - Transfection and plasmids
  - SUMO4 plasmids
  - SUMO2 plasmids
  - SENP1 plasmids
  - RAP80, BRCC36, and Abraxas plasmids
  - SIM-peptide pull-down assay
  - Vinyl-sulfone labeling and turnover kinetics
  - Metaphase spreads
  - Purification of recombinant proteins
- [QUANTIFICATION AND STATISTICAL ANALYSIS](#)
  - Statistics

### SUPPLEMENTAL INFORMATION

Supplemental information can be found online at <https://doi.org/10.1016/j.molcel.2025.02.004>.

Received: December 19, 2022  
Revised: September 27, 2024  
Accepted: February 5, 2025  
Published: March 6, 2025

## REFERENCES

- Pichler, A., Fatouros, C., Lee, H., and Eisenhardt, N. (2017). SUMO conjugation - a mechanistic view. *Biomol. Concepts* 8, 13–36. <https://doi.org/10.1515/bmc-2016-0030>.
- Garvin, A.J., Lanz, A.J., and Morris, J.R. (2022). SUMO monoclonal antibodies vary in sensitivity, specificity, and ability to detect types of SUMO conjugate. *Sci. Rep.* 12, 21343. <https://doi.org/10.1038/s41598-022-25665-6>.
- Wang, H., Yang, L., Wang, Y., Chen, L., Li, H., and Xie, Z. (2019). RPFdb v2.0: an updated database for genome-wide information of translated mRNA generated from ribosome profiling. *Nucleic Acids Res.* 47, D230–D234. <https://doi.org/10.1093/nar/gky978>.
- Galisson, F., Mahrouche, L., Courcelles, M., Bonneil, E., Meloche, S., Chelbi-Alix, M.K., and Thibault, P. (2011). A novel proteomics approach to identify SUMOylated proteins and their modification sites in human cells. *Mol. Cell. Proteomics* 10, M110.004796. <https://doi.org/10.1074/mcp.M110.004796>.
- Lumpkin, R.J., Gu, H., Zhu, Y., Leonard, M., Ahmad, A.S., Clauser, K.R., Meyer, J.G., Bennett, E.J., and Komives, E.A. (2017). Site-specific identification and quantitation of endogenous SUMO modifications under native conditions. *Nat. Commun.* 8, 1171. <https://doi.org/10.1038/s41467-017-01271-3>.
- Lamoliatte, F., McManus, F.P., Maarifi, G., Chelbi-Alix, M.K., and Thibault, P. (2017). Uncovering the SUMOylation and ubiquitylation crosstalk in human cells using sequential peptide immunopurification. *Nat. Commun.* 8, 14109. <https://doi.org/10.1038/ncomms14109>.
- Kunz, K., Piller, T., and Müller, S. (2018). SUMO-specific proteases and isopeptidases of the SENP family at a glance. *J. Cell Sci.* 131, jcs211904. <https://doi.org/10.1242/jcs.211904>.
- Owerbach, D., McKay, E.M., Yeh, E.T.H., Gabbay, K.H., and Bohren, K.M. (2005). A proline-90 residue unique to SUMO-4 prevents maturation and sumoylation. *Biochem. Biophys. Res. Commun.* 337, 517–520. <https://doi.org/10.1016/j.bbrc.2005.09.090>.
- Wei, W.Z., Yang, P., Pang, J.F., Zhang, S., Wang, Y., Wang, M.H., Dong, Z., She, J.X., and Wang, C.Y. (2008). A stress-dependent SUMO4 sumoylation of its substrate proteins. *Biochem. Biophys. Res. Commun.* 375, 454–459. <https://doi.org/10.1016/j.bbrc.2008.08.028>.
- Ma, X.C., Yang, T., Luo, Y.W., Wu, L.Y., Jiang, Y.W., Song, Z., Pan, T., Liu, B.F., Liu, G.Y., Liu, J., et al. (2019). TRIM28 promotes HIV-1 latency by SUMOylating CDK9 and inhibiting P-TEFb. *eLife* 8, e42426. <https://doi.org/10.7554/eLife.42426>.
- Guo, D., Han, J., Adam, B.L., Colburn, N.H., Wang, M.H., Dong, Z., Eizirik, D.L., She, J.X., and Wang, C.Y. (2005). Proteomic analysis of SUMO4 substrates in HEK293 cells under serum starvation-induced stress. *Biochem. Biophys. Res. Commun.* 337, 1308–1318. <https://doi.org/10.1016/j.bbrc.2005.09.191>.
- Morris, J.R., and Garvin, A.J. (2017). SUMO in the DNA Double-Stranded Break Response: Similarities, Differences, and Cooperation with Ubiquitin. *J. Mol. Biol.* 429, 3376–3387. <https://doi.org/10.1016/j.jmb.2017.05.012>.
- Mendes, A.V., Grou, C.P., Azevedo, J.E., and Pinto, M.P. (2016). Evaluation of the activity and substrate specificity of the human SENP family of SUMO proteases. *Biochim. Biophys. Acta* 1863, 139–147. <https://doi.org/10.1016/j.bbamcr.2015.10.020>.
- Shin, E.J., Shin, H.M., Nam, E., Kim, W.S., Kim, J.H., Oh, B.H., and Yun, Y. (2012). DeSUMOylating isopeptidase: a second class of SUMO protease. *EMBO Rep.* 13, 339–346. <https://doi.org/10.1038/embor.2012.3>.
- Schulz, S., Chachami, G., Kozackiewicz, L., Winter, U., Stankovic-Valentin, N., Haas, P., Hofmann, K., Urlaub, H., Ovaia, H., Wittbrodt, J., et al. (2012). Ubiquitin-specific protease-like 1 (USPL1) is a SUMO isopeptidase with essential, non-catalytic functions. *EMBO Rep.* 13, 930–938. <https://doi.org/10.1038/embor.2012.125>.
- Schwertman, P., Bekker-Jensen, S., and Mailand, N. (2016). Regulation of DNA double-strand break repair by ubiquitin and ubiquitin-like modifiers. *Nat. Rev. Mol. Cell Biol.* 17, 379–394. <https://doi.org/10.1038/nrm.2016.58>.
- Garvin, A.J., and Morris, J.R. (2017). SUMO, a small, but powerful, regulator of double-strand break repair. *Philos. Trans. R. Soc. Lond. B Biol. Sci.* 372, 20160281. <https://doi.org/10.1098/rstb.2016.0281>.
- Dhingra, N., and Zhao, X. (2019). Intricate SUMO-based control of the homologous recombination machinery. *Genes Dev.* 33, 1346–1354. <https://doi.org/10.1101/gad.328534.119>.
- Garvin, A.J., Densham, R.M., Blair-Reid, S.A., Pratt, K.M., Stone, H.R., Weekes, D., Lawrence, K.J., and Morris, J.R. (2013). The deSUMOylase SENP7 promotes chromatin relaxation for homologous recombination DNA repair. *EMBO Rep.* 14, 975–983. <https://doi.org/10.1038/embor.2013.141>.
- Garvin, A.J. (2019). Beyond reversal: ubiquitin and ubiquitin-like proteases and the orchestration of the DNA double strand break repair response. *Biochem. Soc. Trans.* 47, 1881–1893. <https://doi.org/10.1042/BST20190534>.
- Galanty, Y., Belotserkovskaya, R., Coates, J., Polo, S., Miller, K.M., and Jackson, S.P. (2009). Mammalian SUMO E3-ligases PIAS1 and PIAS4 promote responses to DNA double-strand breaks. *Nature* 462, 935–939. <https://doi.org/10.1038/nature08657>.
- Ismail, I.H., Gagné, J.P., Caron, M.C., McDonald, D., Xu, Z., Masson, J.Y., Poirier, G.G., and Hendzel, M.J. (2012). CBX4-mediated SUMO modification regulates BMI1 recruitment at sites of DNA damage. *Nucleic Acids Res.* 40, 5497–5510. <https://doi.org/10.1093/nar/gks222>.
- Morris, J.R., Boutell, C., Keppler, M., Densham, R., Weekes, D., Alamshah, A., Butler, L., Galanty, Y., Pangon, L., Kiuchi, T., et al. (2009). The SUMO modification pathway is involved in the BRCA1 response to genotoxic stress. *Nature* 462, 886–890. <https://doi.org/10.1038/nature08593>.
- Danielsen, J.R., Povlsen, L.K., Villumsen, B.H., Streicher, W., Nilsson, J., Wikström, M., Bekker-Jensen, S., and Mailand, N. (2012). DNA damage-inducible SUMOylation of HERC2 promotes RNF8 binding via a novel SUMO-binding zinc finger. *J. Cell Biol.* 197, 179–187. <https://doi.org/10.1083/jcb.201106152>.
- Diehl, C., Akke, M., Bekker-Jensen, S., Mailand, N., Streicher, W., and Wikström, M. (2016). Structural Analysis of a Complex between Small Ubiquitin-like Modifier 1 (SUMO1) and the ZZ Domain of CREB-binding Protein (CBP/p300) Reveals a New Interaction Surface on SUMO. *J. Biol. Chem.* 291, 12658–12672. <https://doi.org/10.1074/jbc.M115.711325>.
- Guzzo, C.M., Ringel, A., Cox, E., Uzoma, I., Zhu, H., Blackshaw, S., Wolberger, C., and Matunis, M.J. (2014). Characterization of the SUMO-binding activity of the myeloproliferative and mental retardation (MYM)-type zinc fingers in ZNF261 and ZNF198. *PLoS ONE* 9, e105271. <https://doi.org/10.1371/journal.pone.0105271>.
- Lee, D., Apelt, K., Lee, S.O., Chan, H.R., Luijsterburg, M.S., Leung, J.W.C., and Miller, K.M. (2022). ZMYM2 restricts 53BP1 at DNA double-strand breaks to favor BRCA1 loading and homologous recombination. *Nucleic Acids Res.* 50, 3922–3943. <https://doi.org/10.1093/nar/gkac160>.
- Yin, Y.L., Seifert, A., Chua, J.S., Maure, J.F., Golebiowski, F., and Hay, R.T. (2012). SUMO-targeted ubiquitin E3 ligase RNF4 is required for the response of human cells to DNA damage. *Genes Dev.* 26, 1196–1208. <https://doi.org/10.1101/gad.189274.112>.
- Galanty, Y., Belotserkovskaya, R., Coates, J., and Jackson, S.P. (2012). RNF4, a SUMO-targeted ubiquitin E3 ligase, promotes DNA double-strand

- break repair. *Genes Dev.* 26, 1179–1195. <https://doi.org/10.1101/gad.188284.112>.
30. Luo, K., Zhang, H., Wang, L., Yuan, J., and Lou, Z. (2012). Sumoylation of MDC1 is important for proper DNA damage response. *EMBO J.* 31, 3008–3019. <https://doi.org/10.1038/emboj.2012.158>.
  31. Vyas, R., Kumar, R., Clermont, F., Helfricht, A., Kalev, P., Sotiropoulou, P., Hendriks, I.A., Radaelli, E., Hocheplied, T., Blanpain, C., et al. (2013). RNF4 is required for DNA double-strand break repair in vivo. *Cell Death Differ.* 20, 490–502. <https://doi.org/10.1038/cdd.2012.145>.
  32. Kumar, R., González-Prieto, R., Xiao, Z., Verlaan-de Vries, M., and Vertegaal, A.C.O. (2017). The STUbL RNF4 regulates protein group SUMOylation by targeting the SUMO conjugation machinery. *Nat. Commun.* 8, 1809. <https://doi.org/10.1038/s41467-017-01900-x>.
  33. Garvin, A.J., Walker, A.K., Densham, R.M., Chauhan, A.S., Stone, H.R., Mackay, H.L., Jamshad, M., Starowicz, K., Daza-Martin, M., Ronson, G.E., et al. (2019). The deSUMOylase SENP2 coordinates homologous recombination and nonhomologous end joining by independent mechanisms. *Genes Dev.* 33, 333–347. <https://doi.org/10.1101/gad.321125.118>.
  34. Psakhye, I., and Jentsch, S. (2012). Protein group modification and synergy in the SUMO pathway as exemplified in DNA repair. *Cell* 151, 807–820. <https://doi.org/10.1016/j.cell.2012.10.021>.
  35. Hendriks, I.A., and Vertegaal, A.C.O. (2016). A comprehensive compilation of SUMO proteomics. *Nat. Rev. Mol. Cell Biol.* 17, 581–595. <https://doi.org/10.1038/nrm.2016.81>.
  36. Pfeiffer, A., Luijsterburg, M.S., Acs, K., Wiegant, W.W., Helfricht, A., Herzog, L.K., Minoia, M., Böttcher, C., Salomons, F.A., van Attikum, H., and Dantuma, N.P. (2017). Ataxin-3 consolidates the MDC1-dependent DNA double-strand break response by counteracting the SUMO-targeted ubiquitin ligase RNF4. *EMBO J.* 36, 1066–1083. <https://doi.org/10.15252/emboj.201695151>.
  37. González-Prieto, R., Cuijpers, S.A.G., Luijsterburg, M.S., van Attikum, H., and Vertegaal, A.C.O. (2015). SUMOylation and PARYlation cooperate to recruit and stabilize SLX4 at DNA damage sites. *EMBO Rep.* 16, 512–519. <https://doi.org/10.15252/embr.201440017>.
  38. Guervilly, J.H., Takedachi, A., Naim, V., Scaglione, S., Chawhan, C., Lovera, Y., Despras, E., Kuraoka, I., Kannouche, P., Rosselli, F., and Gaillard, P.H. (2015). The SLX4 complex is a SUMO E3 ligase that impacts on replication stress outcome and genome stability. *Mol. Cell* 57, 123–137. <https://doi.org/10.1016/j.molcel.2014.11.014>.
  39. Dou, H., Huang, C., Singh, M., Carpenter, P.B., and Yeh, E.T.H. (2010). Regulation of DNA repair through deSUMOylation and SUMOylation of replication protein A complex. *Mol. Cell* 39, 333–345. <https://doi.org/10.1016/j.molcel.2010.07.021>.
  40. Hariharasudhan, G., Jeong, S.Y., Kim, M.J., Jung, S.M., Seo, G., Moon, J.R., Lee, S., Chang, I.Y., Kee, Y., You, H.J., and Lee, J.H. (2022). TOPORS-mediated RAD51 SUMOylation facilitates homologous recombination repair. *Nucleic Acids Res.* 50, 1501–1516. <https://doi.org/10.1093/nar/gkac009>.
  41. Cabello-Lobato, M.J., Jenner, M., Cisneros-Aguirre, M., Brüninghoff, K., Sandy, Z., da Costa, I.C., Jowitt, T.A., Loch, C.M., Jackson, S.P., Wu, Q., et al. (2022). Microarray screening reveals two non-conventional SUMO-binding modules linked to DNA repair by non-homologous end-joining. *Nucleic Acids Res.* 50, 4732–4754. <https://doi.org/10.1093/nar/gkac237>.
  42. González-Prieto, R., Eifler-Olivi, K., Claessens, L.A., Willemstein, E., Xiao, Z., Talavera Ormeno, C.M.P., Ovaa, H., Ulrich, H.D., and Vertegaal, A.C.O. (2021). Global non-covalent SUMO interaction networks reveal SUMO-dependent stabilization of the non-homologous end joining complex. *Cell Rep.* 34, 108691. <https://doi.org/10.1016/j.celrep.2021.108691>.
  43. Hu, X., Paul, A., and Wang, B. (2012). Rap80 protein recruitment to DNA double-strand breaks requires binding to both small ubiquitin-like modifier (SUMO) and ubiquitin conjugates. *J. Biol. Chem.* 287, 25510–25519. <https://doi.org/10.1074/jbc.M112.374116>.
  44. Guzzo, C.M., Berndsen, C.E., Zhu, J.M., Gupta, V., Datta, A., Greenberg, R.A., Wolberger, C., and Matunis, M.J. (2012). DNA DAMAGE RNF4-Dependent Hybrid SUMO-Ubiquitin Chains Are Signals for RAP80 and Thereby Mediate the Recruitment of BRCA1 to Sites of DNA Damage. *Sci. Signal.* 5, ra88. <https://doi.org/10.1126/scisignal.2003485>.
  45. Hinz, M., Stilmann, M., Arslan, S.Ç., Khanna, K.K., Dittmar, G., and Scheiderei, C. (2010). A cytoplasmic ATM-TRAF6-clAP1 module links nuclear DNA damage signaling to ubiquitin-mediated NF-kappaB activation. *Mol. Cell* 40, 63–74. <https://doi.org/10.1016/j.molcel.2010.09.008>.
  46. Fradet-Turcotte, A., Canny, M.D., Escribano-Díaz, C., Orthwein, A., Leung, C.C.Y., Huang, H., Landry, M.C., Kitevski-LeBlanc, J., Noordermeer, S.M., Sicheri, F., and Durocher, D. (2013). 53BP1 is a reader of the DNA-damage-induced H2A Lys 15 ubiquitin mark. *Nature* 499, 50–54. <https://doi.org/10.1038/nature12318>.
  47. Becker, J.R., Clifford, G., Bonnet, C., Groth, A., Wilson, M.D., and Chapman, J.R. (2021). BARD1 reads H2A lysine 15 ubiquitination to direct homologous recombination. *Nature* 596, 433–437. <https://doi.org/10.1038/s41586-021-03776-w>.
  48. Hu, Q., Botuyan, M.V., Zhao, D., Cui, G., Mer, E., and Mer, G. (2021). Mechanisms of BRCA1-BARD1 nucleosome recognition and ubiquitylation. *Nature* 596, 438–443. <https://doi.org/10.1038/s41586-021-03716-8>.
  49. Maréchal, A., and Zou, L. (2015). RPA-coated single-stranded DNA as a platform for post-translational modifications in the DNA damage response. *Cell Res.* 25, 9–23. <https://doi.org/10.1038/cr.2014.147>.
  50. Maquat, L.E. (2005). Nonsense-mediated mRNA decay in mammals. *J. Cell Sci.* 118, 1773–1776. <https://doi.org/10.1242/jcs.01701>.
  51. Merrill, J.C., Melhuish, T.A., Kagey, M.H., Yang, S.H., Sharrocks, A.D., and Wotton, D. (2010). A role for non-covalent SUMO interaction motifs in Pc2/CBX4 E3 activity. *PLoS ONE* 5, e8794. <https://doi.org/10.1371/journal.pone.0008794>.
  52. Lallemand-Breitenbach, V., and de Thé, H. (2018). PML nuclear bodies: from architecture to function. *Curr. Opin. Cell Biol.* 52, 154–161. <https://doi.org/10.1016/j.ceb.2018.03.011>.
  53. Hattersley, N., Shen, L., Jaffray, E.G., and Hay, R.T. (2011). The SUMO protease SENP6 is a direct regulator of PML nuclear bodies. *Mol. Biol. Cell* 22, 78–90. <https://doi.org/10.1091/mbc.E10-06-0504>.
  54. He, X., Riceberg, J., Soucy, T., Koenig, E., Minissale, J., Gallery, M., Bernard, H., Yang, X., Liao, H., Rabino, C., et al. (2017). Probing the roles of SUMOylation in cancer cell biology by using a selective SAE inhibitor. *Nat. Chem. Biol.* 13, 1164–1171. <https://doi.org/10.1038/nchembio.2463>.
  55. Albrow, V.E., Ponder, E.L., Fasci, D., Békés, M., Deu, E., Salvesen, G.S., and Bogoy, M. (2011). Development of small molecule inhibitors and probes of human SUMO deconjugating proteases. *Chem. Biol.* 18, 722–732. <https://doi.org/10.1016/j.chembiol.2011.05.008>.
  56. Shen, L., Tatham, M.H., Dong, C., Zagórska, A., Naismith, J.H., and Hay, R.T. (2006). SUMO protease SENP1 induces isomerization of the scissile peptide bond. *Nat. Struct. Mol. Biol.* 13, 1069–1077. <https://doi.org/10.1038/nsmb.1172>.
  57. Anamika, and Spyropoulos, L. (2016). Molecular Basis for Phosphorylation-dependent SUMO Recognition by the DNA Repair Protein RAP80. *J. Biol. Chem.* 291, 4417–4428. <https://doi.org/10.1074/jbc.M115.705061>.
  58. Fottner, M., Weyh, M., Gaussmann, S., Schwarz, D., Sattler, M., and Lang, K. (2021). A modular toolbox to generate complex polymeric ubiquitin architectures using orthogonal sortase enzymes. *Nat. Commun.* 12, 6515. <https://doi.org/10.1038/s41467-021-26812-9>.
  59. Her, J., Soo Lee, N., Kim, Y., and Kim, H. (2016). Factors forming the BRCA1-A complex orchestrate BRCA1 recruitment to the sites of DNA damage. *Acta Biochim. Biophys. Sin. (Shanghai)* 48, 658–664. <https://doi.org/10.1093/abbs/gmw047>.
  60. Hu, Y., Scully, R., Sobhian, B., Xie, A., Shestakova, E., and Livingston, D.M. (2011). RAP80-directed tuning of BRCA1 homologous

- recombination function at ionizing radiation-induced nuclear foci. *Genes Dev.* 25, 685–700. <https://doi.org/10.1101/gad.2011011>.
61. Coleman, K.A., and Greenberg, R.A. (2011). The BRCA1-RAP80 complex regulates DNA repair mechanism utilization by restricting end resection. *J. Biol. Chem.* 286, 13669–13680. <https://doi.org/10.1074/jbc.M110.213728>.
  62. Cooper, E.M., Cutcliffe, C., Kristiansen, T.Z., Pandey, A., Pickart, C.M., and Cohen, R.E. (2009). K63-specific deubiquitination by two JAMM/MPN+ complexes: BRISC-associated Brcc36 and proteasomal Poh1. *EMBO J.* 28, 621–631. <https://doi.org/10.1038/emboj.2009.27>.
  63. Wang, B., and Elledge, S.J. (2007). Ubc13/Rnf8 ubiquitin ligases control foci formation of the Rap80/Abraxas/Brc1/Brcc36 complex in response to DNA damage. *Proc. Natl. Acad. Sci. USA* 104, 20759–20763. <https://doi.org/10.1073/pnas.0710061104>.
  64. Wang, B., Matsuoka, S., Ballif, B.A., Zhang, D., Smogorzewska, A., Gygi, S.P., and Elledge, S.J. (2007). Abraxas and RAP80 form a BRCA1 protein complex required for the DNA damage response. *Science* 316, 1194–1198. <https://doi.org/10.1126/science.1139476>.
  65. Liu, Z., Wu, J., and Yu, X. (2007). CCDC98 targets BRCA1 to DNA damage sites. *Nat. Struct. Mol. Biol.* 14, 716–720. <https://doi.org/10.1038/nsmb1279>.
  66. Kim, H., Huang, J., and Chen, J. (2007). CCDC98 is a BRCA1-BRCT domain-binding protein involved in the DNA damage response. *Nat. Struct. Mol. Biol.* 14, 710–715. <https://doi.org/10.1038/nsmb1277>.
  67. Shao, G., Lilli, D.R., Patterson-Fortin, J., Coleman, K.A., Morrissey, D.E., and Greenberg, R.A. (2009). The Rap80-BRCC36 de-ubiquitinating enzyme complex antagonizes RNF8-Ubc13-dependent ubiquitination events at DNA double strand breaks. *Proc. Natl. Acad. Sci. USA* 106, 3166–3171. <https://doi.org/10.1073/pnas.0807485106>.
  68. Wu, Q., Paul, A., Su, D., Mehmood, S., Foo, T.K., Ochi, T., Bunting, E.L., Xia, B., Robinson, C.V., Wang, B., and Blundell, T.L. (2016). Structure of BRCA1-BRCT/Abraxas Complex Reveals Phosphorylation-Dependent BRCT Dimerization at DNA Damage Sites. *Mol. Cell* 61, 434–448. <https://doi.org/10.1016/j.molcel.2015.12.017>.
  69. Gareau, J.R., and Lima, C.D. (2010). The SUMO pathway: emerging mechanisms that shape specificity, conjugation and recognition. *Nat. Rev. Mol. Cell Biol.* 11, 861–871. <https://doi.org/10.1038/nrm3011>.
  70. Oka, Y., Bekker-Jensen, S., and Mailand, N. (2015). Ubiquitin-like protein UBL5 promotes the functional integrity of the Fanconi anemia pathway. *EMBO J.* 34, 1385–1398. <https://doi.org/10.15252/emboj.201490376>.
  71. Feng, L., Wang, J., and Chen, J. (2010). The Lys63-specific deubiquitinating enzyme BRCC36 is regulated by two scaffold proteins localizing in different subcellular compartments. *J. Biol. Chem.* 285, 30982–30988. <https://doi.org/10.1074/jbc.M110.135392>.
  72. Ng, H.M., Wei, L.Z., Lan, L., and Huen, M.S.Y. (2016). The Lys(63)-deubiquitylating Enzyme BRCC36 Limits DNA Break Processing and Repair. *J. Biol. Chem.* 291, 16197–16207. <https://doi.org/10.1074/jbc.M116.731927>.
  73. Soo Lee, N., Jin Chung, H., Kim, H.J., Yun Lee, S., Ji, J.H., Seo, Y., Hun Han, S., Choi, M., Yun, M., Lee, S.G., et al. (2016). TRAI/RNF206 is required for recruitment of RAP80 to sites of DNA damage. *Nat. Commun.* 7, 10463. <https://doi.org/10.1038/ncomms10463>.
  74. Lombardi, P.M., Matunis, M.J., and Wolberger, C. (2017). RAP80, ubiquitin and SUMO in the DNA damage response. *J. Mol. Med. (Berl.)* 95, 799–807. <https://doi.org/10.1007/s00109-017-1561-1>.
  75. Wu, J., Huen, M.S.Y., Lu, L.Y., Ye, L., Dou, Y., Ljungman, M., Chen, J., and Yu, X. (2009). Histone ubiquitination associates with BRCA1-dependent DNA damage response. *Mol. Cell Biol.* 29, 849–860. <https://doi.org/10.1128/MCB.01302-08>.
  76. Strauss, C., Halevy, T., Macarov, M., Argaman, L., and Goldberg, M. (2011). MDC1 is ubiquitinated on its tandem BRCT domain and directly binds RAP80 in a UBC13-dependent manner. *DNA Repair* 10, 806–814. <https://doi.org/10.1016/j.dnarep.2011.04.016>.
  77. Liebelt, F., Jansen, N.S., Kumar, S., Gracheva, E., Claessens, L.A., Verlaan-de Vries, M., Willemstein, E., and Vertegaal, A.C.O. (2019). The poly-SUMO2/3 protease SENP6 enables assembly of the constitutive centromere-associated network by group deSUMOylation. *Nat. Commun.* 10, 3987. <https://doi.org/10.1038/s41467-019-11773-x>.
  78. Wagner, K., Kunz, K., Piller, T., Tascher, G., Hölper, S., Stehmeier, P., Keiten-Schmitz, J., Schick, M., Keller, U., and Müller, S. (2019). The SUMO Isopeptidase SENP6 Functions as a Rheostat of Chromatin Residency in Genome Maintenance and Chromosome Dynamics. *Cell Rep.* 29, 480–494.e5. <https://doi.org/10.1016/j.celrep.2019.08.106>.
  79. Kukkula, A., Ojala, V.K., Mendez, L.M., Sistonen, L., Elenius, K., and Sundvall, M. (2021). Therapeutic Potential of Targeting the SUMO Pathway in Cancer. *Cancers (Basel)* 13, 4402. <https://doi.org/10.3390/cancers13174402>.
  80. Brand, M., Bommeli, E.B., Rütimann, M., Lindenmann, U., and Riedl, R. (2022). Discovery of a Dual SENP1 and SENP2 Inhibitor. *Int. J. Mol. Sci.* 23, 12085. <https://doi.org/10.3390/ijms232012085>.
  81. Desiere, F., Deutsch, E.W., King, N.L., Nesvizhskii, A.I., Mallick, P., Eng, J., Chen, S., Eddes, J., Loevenich, S.N., and Aebersold, R. (2006). The PeptideAtlas project. *Nucleic Acids Res.* 34, D655–D658. <https://doi.org/10.1093/nar/gkj040>.
  82. Densham, R.M., Garvin, A.J., Stone, H.R., Strachan, J., Baldock, R.A., Daza-Martin, M., Fletcher, A., Blair-Reid, S., Beesley, J., Johal, B., et al. (2016). Human BRCA1-BARD1 ubiquitin ligase activity counteracts chromatin barriers to DNA resection. *Nat. Struct. Mol. Biol.* 23, 647–655. <https://doi.org/10.1038/nsmb.3236>.
  83. Gunn, A., and Stark, J.M. (2012). I-SceI-based assays to examine distinct repair outcomes of mammalian chromosomal double strand breaks. *Methods Mol. Biol.* 920, 379–391. [https://doi.org/10.1007/978-1-61779-998-3\\_27](https://doi.org/10.1007/978-1-61779-998-3_27).
  84. Butler, L.R., Densham, R.M., Jia, J., Garvin, A.J., Stone, H.R., Shah, V., Weekes, D., Festy, F., Beesley, J., and Morris, J.R. (2012). The proteasomal de-ubiquitinating enzyme POH1 promotes the double-strand DNA break response. *EMBO J.* 31, 3918–3934. <https://doi.org/10.1038/emboj.2012.232>.
  85. Schindelin, J., Rueden, C.T., Hiner, M.C., and Eliceiri, K.W. (2015). The ImageJ ecosystem: an open platform for biomedical image analysis. *Mol. Reprod. Dev.* 82, 518–529. <https://doi.org/10.1002/mrd.22489>.
  86. Aitken, A., and Learmonth, M. (2002). Protein identification by in-gel digestion and mass spectrometric analysis. *Mol. Biotechnol.* 20, 95–97. <https://doi.org/10.1385/MB:20:1:095>.
  87. Rueden, C.T., Schindelin, J., Hiner, M.C., DeZonia, B.E., Walter, A.E., Arena, E.T., and Eliceiri, K.W. (2017). ImageJ2: ImageJ for the next generation of scientific image data. *BMC Bioinformatics* 18, 529. <https://doi.org/10.1186/s12859-017-1934-z>.

STAR★METHODS

KEY RESOURCES TABLE

REAGENT or RESOURCE	SOURCE	IDENTIFIER
<b>Antibodies</b>		
FLAG (Goat Polyclonal)	Abcam	Cat# ab1257; RRID:AB_299216
FLAG M2 (Mouse Monoclonal)	SIGMA	Cat# F1804; RRID:AB_262044
GAPDH 6C5 (Mouse Monoclonal)	Calbiochem	Cat# CB1001; RRID:AB_2107426
HA.11 (Mouse Monoclonal)	Biolegend	Cat# 901501; RRID:AB_2565006
53BP1 (Goat Polyclonal)	R&D Systems	Cat# AF1877; RRID:AB_2206635
53BP1 (Rabbit Polyclonal)	Abcam	Cat# ab36823; RRID:AB_722497
PML C7 (Mouse Monoclonal)	Abcam	Cat# ab96051; RRID:AB_10679887
PML (Rabbit Polyclonal)	Invitrogen	Cat# PA5-79835; RRID:AB_2746950
SENP1 (Rabbit Polyclonal)	Abcam	Cat# ab108981; RRID:AB_10862449
SENP2 (Rabbit Monoclonal)	Abcam	Cat# ab124724; RRID:AB_10972485
SENP3 (Rabbit Monoclonal)	Abcam	Cat# ab124790; RRID:AB_10974596
SENP5 (Rabbit Polyclonal)	Abcam	Cat# ab58420; RRID:AB_882487
SENP6 (Rabbit Polyclonal)	Atlas	Cat# HPA024376; RRID:AB_1856678
SENP7 (Rabbit Polyclonal)	Atlas	Cat# HPA027259; RRID:AB_1856679
SUMO1 Y299 (Rabbit Monoclonal)	Abcam	Cat# ab32058; RRID:AB_778173
SUMO1 21C7 (Mouse Monoclonal)	Invitrogen	Cat# 33-2400; RRID:AB_2533109
SUMO2/3 8A2 (Mouse Monoclonal)	Abcam	Cat# ab81371; RRID:AB_1658424
SUMO2/3 12F3 (Mouse Monoclonal)	Cytoskeleton	Cat# ASM23; RRID:AB_2884967
H2AX-pSer139 (Mouse Monoclonal)	Abcam	Cat# ab2893; RRID:AB_303388
H2AX-pSer139 (Rabbit Polyclonal)	Abcam	Cat# ab22551; RRID:AB_447150
MDC1 (Rabbit Polyclonal)	Bethyl	Cat# PLA-0016
MYC 9E10 (Mouse Monoclonal)	Abcam	Cat# ab32; RRID:AB_303599
Vinculin (Rabbit Monoclonal)	Abcam	Cat# ab129002; RRID:AB_11144129
BARD1 (Rabbit Polyclonal)	Abcam	Cat# ab226854
RPA32-pSer33 (Rabbit Polyclonal)	Abcam	Cat# ab211877; RRID:AB_2818947
RAD51 (Rabbit Polyclonal)	Calbiochem	Cat# PC130; RRID:AB_2238184
SP100 (Rabbit Polyclonal)	Atlas	Cat# HPA017384; RRID:AB_1857399
RAP80 (Rabbit Polyclonal)	Novus	Cat# NBP1-87156; RRID:AB_10999813
RAP80 (Rabbit Polyclonal)	Abcam	Cat# ab124763; RRID:AB_10972663
RNF168 (Rabbit Polyclonal)	Abcam	Cat# ab220324.
RNF8 (Rabbit Monoclonal)	Abcam	Cat# ab128872; RRID:AB_11140853
PIAS4 (Mouse Monoclonal)	Abcam	Cat# ab211625
UBC9 (Rabbit Monoclonal)	Abcam	Cat# ab75854; RRID:AB_1310787
UBC13 (Rabbit Polyclonal)	CST	Cat# 4919; RRID:AB_2211168
BRCA2 (Mouse Monoclonal)	Merck	Cat# OP95; RRID:AB_2067762
PIAS1 (Rabbit Monoclonal)	Abcam	Cat# ab109388; RRID:AB_10867435
TAB2 (Rabbit Polyclonal)	Bethyl	Cat# A302-759A; RRID:AB_10630603
PIAS3 (Rabbit Polyclonal)	Abcam	Cat# ab221901
SENP1 (aa578-590, Rabbit Polyclonal)	Novus	Cat# NB100-56405; RRID:AB_2186275
RFP (Mouse Monoclonal 6G6)	Chromotek	Cat# 6g6-100; RRID: AB_2631395
SUMO2/3/4 IOO-19 (Rabbit Monoclonal)	Abnova	Cat# MAB20759
Poly-Histidine (Mouse Monoclonal HIS-1)	Merck	Cat# H1029; AB_260015
Goat $\alpha$ Mouse AF 488	LifeTech	Cat# A11001; RRID:AB_2534069

(Continued on next page)

**Continued**

REAGENT or RESOURCE	SOURCE	IDENTIFIER
Goat $\alpha$ Rabbit AF 488	LifeTech	Cat# A11008; RRID:AB_143165
Goat $\alpha$ Mouse AF 555	LifeTech	Cat# A21422; RRID:AB_141822
Goat $\alpha$ Rabbit AF 555	LifeTech	Cat# A21428; RRID:AB_2535849
Rabbit $\alpha$ Mouse HRP	DAKO	Cat# P0161; RRID:AB_2687969
Swine $\alpha$ Rabbit HRP	DAKO	Cat# P0217; RRID:AB_2728719

**Bacterial and virus strains**

DH5 $\alpha$ Gold	New England Biolabs	Cat# C29871
BL21 DE3	New England Biolabs	Cat# C2527H

**Chemicals, peptides, and recombinant proteins**

Camptothecin (CPT)	Merck	Cat# 208925
Doxycycline	Merck	Cat# D9891
Cisplatin	Selleck	Cat# S1166
Olaparib	Selleck	Cat# S1060
Hygromycin B	Invitrogen	Cat# H044-81VS
Iodoacetamide (IAA)	Merck	Cat# I1149
ML-792	Selleck	Cat# S8697
2-D08	Merck	Cat# SML1052-5MG
EdU	Merck	Cat# 900584-50MG
Karyomax (Colcemid)	Gibco	Cat# 15212012
PIAS1 SIM peptide (Biotin-NKKVEVI DLTIDSSSDEEEEE)	GenScript	N/A
SLX4 SIM peptide (Biotin-LNEEDEV ILLDSDEELE)	GenScript	N/A
SUMO4 WT (aa1-95)	Garvin et al. <sup>2</sup>	N/A
SUMO4 QFI-A (aa1-95)	This study	N/A
ProSUMO3 WT (aa1-103)	Garvin et al. <sup>2</sup>	N/A
diSUMO2 (2-8)	R&D Systems	Cat# ULC-200-050
SUMO1 WT (aa1-95)	Garvin et al. <sup>2</sup>	N/A
RANGAP1 (aa398-587)	This study	N/A
SENP1 catalytic domain	R&D Systems	Cat# E-700-050
HA-SUMO1-Vinyl Sulfone	R&D Systems	Cat# UL-703-050
HA-SUMO2-Vinyl Sulfone	R&D Systems	Cat# UL-759-050
Eukitt mounting media	Sigma	Cat# 03989
Giemsa stain	Sigma	Cat# GS500
bis[sulfosuccinimidyl] suberate (BS <sup>3</sup> )	Fisher	Cat# A39266
Magna-Bind Streptavidin Beads	Thermo Scientific	Cat# 21344

**Deposited data**

Immunoblots, images and raw data (counts) for graphs.	This study; Mendeley Data. Figures and <a href="#">Figures S1–S4</a>	Mendeley: doi: <a href="https://doi.org/10.17632/8s2rtcgw8.1">https://doi.org/10.17632/8s2rtcgw8.1</a>
Immunoblots, images and raw data (counts) for graphs.	This study; Mendeley Data. Figures and <a href="#">Figures S5 and S6</a>	Mendeley: doi: <a href="https://doi.org/10.17632/k7sfchtv83.1">https://doi.org/10.17632/k7sfchtv83.1</a>
Images	This study; Mendeley Data. <a href="#">Figure S6</a> images.	Mendeley: doi: <a href="https://doi.org/10.17632/9syc9p829m.1">https://doi.org/10.17632/9syc9p829m.1</a>
Mass spectrometry data was deposited to the ProteomeXchange Consortium via the PRIDE partner repository ( <a href="https://www.ebi.ac.uk/pride/">https://www.ebi.ac.uk/pride/</a> )	This study.	ProteomeXchange: dataset identifier PXD054695 and <a href="https://doi.org/10.6019/PXD054695">https://doi.org/10.6019/PXD054695</a> .

(Continued on next page)

**Continued**

REAGENT or RESOURCE	SOURCE	IDENTIFIER
Experimental models: Cell lines		
U2OS FlpIn TREx	Garvin et al. <sup>2</sup>	N/A
HeLa FlpIn TREx	Densham et al. <sup>82</sup>	N/A
NCI-H1299	ATCC	Cat# CRL-5803; CVCL_0060
U2OS DR3	Gunn et al. <sup>83</sup>	N/A
U2OS EJ5	Gunn et al. <sup>83</sup>	N/A
U2OS FlpIn 6xHis-HA SUMO4 WT	This study	N/A
U2OS FlpIn 6xHis-HA SUMO4 QFI-A	This study	N/A
U2OS FlpIn 6xHis-HA SUMO4 T91X	This study	N/A
U2OS FlpIn 6xHis-HA SUMO4 G92A/G93A	This study	N/A
U2OS FlpIn 6xHis-HA SUMO4 P90Q	This study	N/A
U2OS FlpIn 6xHis-HA SUMO4 V94X	This study	N/A
U2OS FlpIn 6xHis-HA SUMO4 G92A/G93A/V94X	This study	N/A
U2OS FlpIn SUMO4 KO cl.1.11	This study	N/A
U2OS FlpIn SUMO4 KO cl.4.57	This study	N/A
U2OS FlpIn SUMO4 KO cl.1.11 FLAG-HA SUMO4 WT	This study	N/A
U2OS FlpIn SUMO4 KO cl.1.11 FLAG-HA SUMO4 QFI-A	This study	N/A
U2OS FlpIn SUMO4 KO cl.1.11 FLAG-HA SUMO4 T91X	This study	N/A
U2OS FlpIn SUMO4 KO cl.1.11 FLAG-HA SUMO4 G92A/G93A	This study	N/A
U2OS FlpIn SUMO4 KO cl.1.11 FLAG-HA SUMO4 P90Q	This study	N/A
U2OS FlpIn SUMO4 KO cl.1.11 FLAG-HA SUMO4 V94X	This study	N/A
U2OS FlpIn SUMO4 KO cl.1.11 FLAG-HA SUMO4 G92A/G93A/V94X	This study	N/A
U2OS FlpIn SUMO4 KO cl.1.11 6xHis-HA SUMO4 WT	This study	N/A
U2OS FlpIn SUMO4 KO cl.1.11 6xHis-myc SUMO2 GA	This study	N/A
U2OS FlpIn myc RNF168 WT	This study	N/A
U2OS FlpIn FLAG SENP1 WT	This study	N/A
U2OS FlpIn FLAG SENP1 C603A	This study	N/A
U2OS FlpIn myc RAP80 WT	This study	N/A
U2OS FlpIn myc RAP80 SIM (F40A/V41A/I42A)	This study	N/A
U2OS FlpIn 6xHis-FLAG SUMO2 K11R	This study	N/A
U2OS FlpIn 6xHis-FLAG SUMO2 K21R	This study	N/A
U2OS FlpIn SUMO4 KO cl.1.11 6xHis-FLAG SUMO2 K11R	This study	N/A
U2OS FlpIn SUMO4 KO cl.1.11 6xHis-FLAG SUMO2 K21R	This study	N/A
U2OS FlpIn FLAG Abraxas WT	This study	N/A
U2OS FlpIn FLAG Abraxas S404A/S406A	This study	N/A
U2OS FlpIn HA BRCC36 WT	This study	N/A
U2OS FlpIn HA BRCC36 H124Q/H126Q	This study	N/A
U2OS FlpIn SUMO4 KO cl.1.11 FLAG Abraxas WT	This study	N/A

(Continued on next page)

**Continued**

REAGENT or RESOURCE	SOURCE	IDENTIFIER
U2OS FlpIn SUMO4 KO cl.1.11 FLAG Abraxas S404A/S406A	This study	N/A
U2OS FlpIn SUMO4 KO cl.1.11 HA BRCC36 WT	This study	N/A
U2OS FlpIn SUMO4 KO cl.1.11 HA BRCC36 H124Q/H126Q	This study	N/A
<b>Oligonucleotides</b>		
All oligonucleotide sequences:	This study	<a href="#">Table S4</a>
<b>Recombinant DNA</b>		
pOG44	Invitrogen/Thermo Fisher	V600520
Scel	Gunn et al. <sup>83</sup>	N/A
pcDNA3.1 mRFP	Butler et al. <sup>84</sup>	N/A
pCDNA5/FRT/TO Myc-RNF168 WT	Garvin et al. <sup>33</sup>	n/A
pSpCas9 (BB)-2A PURO gRNA 1	GenScript	Cat#SC1678
pSpCas9 (BB)-2A PURO gRNA 4	GenScript	Cat#SC1678
pCDNA5/FRT/TO 6xHis-HA SUMO4 WT	GenScript	N/A
pCDNA5/FRT/TO 6xHis-HA SUMO4 WT siR	Garvin et al. <sup>2</sup>	N/A
pCDNA5/FRT/TO 6xHis-HA SUMO4 WT T91X siR	GenScript	N/A
pCDNA5/FRT/TO 6xHis-HA SUMO4 WT G92A/G93A siR	GenScript	N/A
pCDNA5/FRT/TO 6xHis-HA SUMO4 WT P90Q siR	GenScript	N/A
pCDNA5/FRT/TO 6xHis-HA SUMO4 WT V94X siR	GenScript	N/A
pCDNA5/FRT/TO 6xHis-HA SUMO4 WT G92A/G93A/V94X siR	GenScript	N/A
pCDNA5/FRT/TO FLAG-HA SUMO4 WT siR	This study	N/A
pCDNA5/FRT/TO FLAG-HA SUMO4 T91X siR	This study	N/A
pCDNA5/FRT/TO FLAG-HA SUMO4 G92A/G93A siR	This study	N/A
pCDNA5/FRT/TO FLAG-HA SUMO4 P90Q siR	This study	N/A
pCDNA5/FRT/TO FLAG-HA SUMO4 V94X siR	This study	N/A
pCDNA5/FRT/TO FLAG-HA SUMO4 G92A/G93A/V94X siR	This study	N/A
pcDNA3.1 mRFP-6xHis-HA SUMO4 WT siR	This study	N/A
pcDNA3.1 mRFP-6xHis-HA SUMO4 V94X siR	This study	N/A
pCDNA5/FRT/TO 6xHis-HA SUMO4 QFI-A siR	This study	N/A
pCDNA5/FRT/TO FLAG-HA SUMO4 QFI-A siR	This study	N/A
pcDNA3.1 mRFP-6xHis-HA SUMO4 QFI-A siR	This study	N/A
pCDNA5/FRT/TO FLAG SENP1 WT siR	GenScript	N/A
pCDNA5/FRT/TO FLAG SENP1 C603A siR	GenScript	N/A
pCDNA5/FRT/TO myc RAP80 WT siR	GenScript	N/A
pCDNA5/FRT/TO myc RAP80 SIM siR	GenScript	N/A
pCDNA5/FRT/TO 6xHis-FLAG SUMO2 K11R	GenScript	N/A
pCDNA5/FRT/TO 6xHis-FLAG SUMO2 K21R	GenScript	N/A
pCDNA5/FRT/TO HA BRCC36 WT siR	GenScript	N/A
pCDNA5/FRT/TO HA BRCC36 HQ siR	GenScript	N/A
pCDNA5/FRT/TO FLAG Abraxas WT siR	GenScript	N/A
pCDNA5/FRT/TO FLAG Abraxas SA siR	GenScript	N/A
pCDNA5/FRT/TO 6xHis-myc SUMO2 G92A/G93A	Garvin et al. <sup>33</sup>	N/A
pET23a-His-RANGAP1 Tail	Frauke Melchior	RRID:Addgene_53139

(Continued on next page)

**Continued**

REAGENT or RESOURCE	SOURCE	IDENTIFIER
pET28a-His-hAos1	Frauke Melchior	RRID:Addgene_53135
pET28b-hUba2-His	Frauke Melchior	RRID:Addgene_53117
p3991 pET ubcH9	Peter Howley	RRID:Addgene_8651
RFP-SUMO3	Morris et al. <sup>23</sup>	N/A
<b>Software and algorithms</b>		
GraphPad Prism 9.2	Graph Pad	9.2.0
ImageJ	Schindelin et al. <sup>85</sup>	<a href="https://imagej.nih.gov/ij/">https://imagej.nih.gov/ij/</a>
FACS software	Backman Coulter	Summit 4.3
Proteome Discoverer 2.5	Thermo Scientific	CSW0064765
Xcalibur	Thermo Scientific	OPTON-30965

**EXPERIMENTAL MODEL AND STUDY PARTICIPANT DETAILS**

**Mammalian cell culture, stable cell lines, and SUMO4<sup>T</sup> cells**

U2OS (female) of HeLa (female) and NCI-H1299 (male) cell lines were cultured in DMEM supplemented with 10% FBS and 1% Penicillin-Streptomycin. FlpIn stable cell lines (bearing SUMO4, SENP1 BRCC36 and Abraxas) were generated using U2OS<sup>TrEx-FlpIn</sup> (a gift from Grant Stewart, University of Birmingham) cells transfected with pcDNA5/FRT/TO-based vectors and the recombinase pOG44 (Invitrogen) using FuGene6 (Promega) at a ratio of 4  $\mu$ l FuGENE / 1  $\mu$ g DNA. After 48 hr, cells were grown in hygromycin selection media (150  $\mu$ g/ml) until colonies formed on plasmid-transfected plates but not controls. Protein expression was induced following 48–72 h induction with doxycycline (1  $\mu$ g ml<sup>-1</sup>) and confirmed by immunoblotting. Details of all cell lines used in this study can be found in the [key resources table](#).

SUMO4 knockout U2OS<sup>TrEx-FlpIn</sup> were generated using two different guide RNAs pSpCas9 (BB)-2A PURO (GenScript) plasmids that target the SUMO4 gene at nucleotides (relative to start codon) 150-171 (gRNA #1) and 186-204 (gRNA #4). For each gRNA, three 10 cm<sup>2</sup> plates of U2OS<sup>TrEx-FlpIn</sup> were transfected at 5  $\mu$ g DNA each, using FuGene6. After 48 hr, cells were treated with puromycin (1  $\mu$ g/mL) to remove un-transfected cells for a further 48 hr. Selected cells were replated at low density on 15 cm<sup>2</sup> plates to allow clonal growth in DMEM without puromycin. After 10 days, clones were re-seeded and expanded. Clones were screened by PCR using primers that flank the SUMO4 gene using genomic DNA purified with direct PCR buffer (Viagen). Clones that displayed reduced size of SUMO4 PCR product were sequenced by Sanger sequencing to confirm disruption of the SUMO4 locus. Western blot with FLAG was used to confirm the presence of stably integrated 3xFlagCas9. Clones that were positive for 3xFLAG-Cas9 were discarded to reduce the possibility of off-target editing by overexpressed Cas9 nuclease. SUMO4<sup>T</sup> clone 1.11 was used for the generation of all complemented cell lines as for the parental U2OS<sup>TrEx-FlpIn</sup> cell line. Cell lines used and generated are listed in the [key resources table](#).

**METHOD DETAILS**

**Transfections**

siRNA transfections were performed using Dharmafect1 (Dharmacon) and DNA plasmids using FuGENE 6 (3  $\mu$ l:1  $\mu$ g FuGENE:DNA) (Promega) following the manufacturer's protocols. Cells were grown for 48 h post transfection before treatment and collection. All siRNA sequences are given in the [key resources table](#).

**Cell cycle analysis**

U2OS were plated directly onto 24 well plates (Corning) and attached overnight prior to siRNA depletion for 72 hours. EdU was then pulsed into cells at a concentration of 1  $\mu$ M per ml for 30 mins before fixation. Cells were directly fixed onto the plate using 4% PFA in PBS for 10 minutes at room temperature, washed in 1x PBS and permeabilized in 0.5% triton for 5 minutes at room temperature. Samples were then blocked in 10% FBS in PBS for 30 mins. Click-iT was performed as detailed in the Click-iT EdU Imaging Kits (Life Technologies). Cells were washed in 1x PBS before incubating with Hoechst for 1 h. Hoechst was removed, and cells were covered with PBS.

Stained plates were imaged on the CellInsight CX5 High-Content Screening (HCS) Platform (ThermoFisher scientific) using the 10x objective and HCS Studio Cell Analysis Software. For each cell the raw values for Total Hoechst intensity and Average EdU intensity were extracted from the CellInsight software so that it could be plotted.

### Non-denaturing SUMO immunoprecipitation

$1 \times 10^6$  U2OS cells were mock transfected, or transfected with plasmids encoding for FLAG-SUMO3, HA-SUMO4, or both plasmids together. After 72 hours, cells were harvested, washed and lysed in IP Buffer (10 mM HEPES-pH 7.6, 200 mM NaCl, 1.5 mM  $MgCl_2$ , 10% glycerol, 0.2 mM EDTA, 1% Triton) supplemented with protease and phosphatase inhibitors. Following sonication, lysates were cleared (12000 Rpm, 10 minutes, 4°C), antibodies (HA or SUMO2/3/4 I00-19) or pre-linked agarose beads (FLAG) added and samples rotated (overnight, 4°C). For HA or SUMO4 IPs, protein A/G agarose beads (ThermoFisher Scientific) were added and samples rotated (30 minutes, 4°C). In all cases, beads were then washed 3 times with ice cold IP buffer, before being eluted in 4x SDS Loading buffer and analysed by Western blot. To prepare samples for LC-MS/MS analysis,  $1.5 \times 10^8$  WT or SUMO4<sup>T</sup> U2OS cells were subjected to the IP protocol as above.

### Proteomics analysis

Coomassie stained bands corresponding to the molecular weight of SUMO4 were excised from a Novex™ 4-20% Tris-Glycine Gel (ThermoFisher scientific). Bands were digested as previously described<sup>86</sup> except 200 mM ammonium bicarbonate (pH 8) was used throughout, there was no reduction step, and the bands are digested with 5 ng/μl LysC at 37°C for 16 hours prior to peptide extraction with 100% acetonitrile. The samples were dried down to remove the acetonitrile and then re-suspended in 0.1% formic acid solution in water prior to LC-MS/MS analysis.

Liquid chromatography-mass spectrometry (LC-MS) analysis was performed on an UltiMate® 3000 HPLC series (Dionex, Sunnyvale, CA USA) coupled to a QExactive HF mass spectrometer (ThermoFisher Scientific). The peptides were trapped on precolumn, Thermo Scientific Acclaim PepMap 100 C18 HPLC Columns, 3 μm particle size, 2 cm length, 75 μm I.D., (Dionex, Sunnyvale, CA USA) and separated using a PepMap 100 analytical column (75 μm I.D. x 15 cm, 3 μm) (Dionex, Sunnyvale, CA USA). The LC system was equilibrated in solvent A (0.1% formic acid in water). The gradient used was from 3.2% to 44% solvent B (0.1% formic acid in 100% acetonitrile) for 30 min to elute the peptides, using a flow rate of 350 nLmin<sup>-1</sup>. All peptides were infused directly into the mass spectrometer via a Triversa Nanomate nanospray source (Advion Biosciences, NY). The capillary voltage was set to 1.7 kV. The mass spectrometer performed a full MS scan ( $m/z$  360–1600) and subsequent HCD MS/MS scans of the 20 most abundant ions with dynamic exclusion setting 15 s. Full scan mass spectra were recorded at a resolution of 120,000 at  $m/z$  200 and AGC target of  $3 \times 10^6$ . For MS/MS, the HCD was set to 28 NCE, Orbitrap resolution to 15,000 and AGC target to  $1 \times 10^5$ . The width of the precursor isolation window was 1.2  $m/z$  and only multiply-charged precursor ions were selected for MS/MS. The MS and MS/MS scans were searched using Protein Discoverer v. 2.5 using the Sequest HT algorithm. A fasta file consisting of SUMO1-4 sequences was used (Table S1). The dynamic modifications were oxidation (Met), N-terminal acetylation and N-terminal met-loss+acetylation, with carbamidomethyl (Cys) set as a fixed modification. The number of missed cleavages set to 3. The precursor mass tolerance was set to 10 ppm and the MS/MS mass tolerance 0.02 Da. The PSMs were validated using fixed value PSM validator mode with only high/medium confidence level peptides reported.

### Immunofluorescence

U2OS were plated at  $2.5 \times 10^4$  cells/well on 13 mm glass coverslips in 24 well plates (Corning) and attached overnight prior to siRNA depletion for 48 hours. For pre-extraction after 1x PBS wash cells were treated with 250 μL / well ice-cold CSK buffer (100 mM NaCl, 300 mM sucrose, 3 mM  $MgCl_2$ , 0.7% Triton-X100 and 10 mM PIPES) for 30 seconds prior to fixation with 4% Paraformaldehyde (PFA) in PBS at room temperature for 10 minutes. For non-pre-extracted samples, cells were fixed in 4% PFA at room temperature for 10 minutes, followed by permeabilization with 0.5% Triton in PBS for 5 minutes. Coverslips were blocked with 5% FBS in PBS for 1 hour at room temperature, followed by incubation with primary antibodies at the concentrations shown in Table S2, overnight at 4°C in 5% FBS. Coverslips were washed twice with PBS followed by incubation with Alexa-Fluor 555 conjugated secondary antibodies at 1:2500 for 2 hours at room temperature in the dark. Cells were washed twice with PBS prior to incubation with 250 μL of Hoechst (1 μg/mL) for 2 minutes. Coverslips were mounted on slides using Immuno-Mount (Thermo Scientific) and sealed. Imaging was carried out on a Leica DM6000B microscope using an HBO lamp with a 100 W mercury short arc UV bulb light source. Images were captured at each wavelength sequentially using the Plan Apochromat HCX 100x/1.4 Oil objective at a resolution of 1392x1040 pixels. For RAD51 staining cells were pulsed with 10 μM EdU 30 min prior to fixation to label S phase cells and dU was visualized by Click-iT chemistry according to the manufacturer's protocols (Life Technologies) with Alexa-647-azide.

### Modified lysis and SDS-PAGE (for SUMO4 separation)

U2OS were seeded in 15 cm<sup>2</sup> dishes and grown to confluency before scraping into suspension in 1XPBS. Cells were pellet with 500g for 10 minutes and then lysed in 10 mM HEPES-pH 7.6, 200 mM NaCl, 1.5 mM  $MgCl_2$ , 10% glycerol, 0.2 mM EDTA, 1% Triton) supplemented with 1xComplete Mini protease inhibitor tablet/2 ml and phosphatase inhibitors, with 4x10 seconds of sonication at 10 kHz with 2 minutes recovery on ice. Lysates were then centrifuged at 13,000g for 5 minutes and the supernatant was combined with 4xLaemmli buffer. Samples were run on a 15% SDS-PAGE gel at 80v for 6-8 hours and transferred to PVDF membrane at 200 mA for 24 hours.

### Cell survival colony assays

Cells plated at  $2 \times 10^5$  per ml were treated as indicated in the figure legends using agents and doses in Table S3. Cells were then trypsinized and plated at limiting dilution to form colonies and grown on for 10–14 days. Colonies were stained using 0.5% crystal violet (BDH Chemicals) in 50% methanol and counted. Each experiment contained three technical repeats, a minimum of three independent experiments and is normalized to untreated controls.

### DNA repair reporter assays

U2OS-DR3-GFP (HR) and U2OS-EJ5-GFP (NHEJ) U2OS reporter cell lines were a generous gift from Jeremy Stark (City of Hope, Duarte USA). Cell lines were transfected with siRNAs using Dharmafect1 (Dharmacon) and DNA (RFP, I-Sce1 endonuclease expression constructs, with or without His-HA-mRFP-SUMO4 variants) using FuGene6 (Promega). After 16 h media was replaced and cells grown for a further 48 h before fixation in 2% paraformaldehyde (PFA). RFP and GFP double positive cells were scored by FACS analysis using a CyAn flow cytometer and a minimum of 10,000 cells counted and data analyzed using Summit 4.3 software. Each individual experiment contained a minimum of three technical repeats and normalized to siRNA controls or to WT-complemented cells.

### Transfection and plasmids

DNA transfections were performed using FuGene6 (Promega) at a ratio of 4  $\mu$ l FuGENE / 1  $\mu$ g DNA on 40% confluent cells. Transfection of siRNAs were typically at 10 nM per sequence (or 5 nM per sequence where two are combined). For dual depletions, a total of 10 nM of each siRNA was used to make 20 nM total. Dharmafect-1 was used at a concentration of 1 mL per mL of media.

### SUMO4 plasmids

6xHis-HA-SUMO4 cDNA (GenBank: NM\_001002255.1) was generated by GenScript to include synonymous mutations that render it insensitive to siRNA #2 and siRNA #3. 6xHis-HA-SUMO4 was subcloned into pcDNA5/FRT/TO using HindIII-BamHI sites. 6xHis-HA-SUMO4 non-siRNA resistant vector contains the original cDNA without siRNA resistance. 6xHis-HA-mRFP-SUMO4 were subcloned from the pcDNA5/FRT/TO vector to pcDNA3.1 mRFP using HindIII - XhoI sites. FLAG-HA-SUMO4 constructs were generated using primers that replaced the 6xHis tag with FLAG epitope and were cloned into pcDNA5/FRT/TO using HindIII - XhoI sites.

### SUMO2 plasmids

6xHis-FLAG SUMO2 K11R and K21R were generated by GenScript and cloned into pcDNA5/FRT/TO at BamHI and XhoI sites.

### SENP1 plasmids

Human SENP1 cDNA (ENST00000448372.5) was synthesized by GenScript to contain an N-terminal FLAG tag and synonymous siRNA resistance mutations to the exon 6 and 12 siRNA used (see [key resources table](#), 'Oligonucleotides'). The cDNA also has synonymous mutations to remove BamHI, XhoI and NcoI sites and is cloned into pcDNA5/FRT/TO using BamHI - XhoI sites.

### RAP80, BRCC36, and Abraxas plasmids

Human RAP80 (also known as UIMC1, ENST00000511320.6) was generated by gene synthesis (GenScript). The cDNA for RAP80 contains an N-terminal myc epitope tag. The RAP80 cDNA contains synonymous mutations to make it resistant to siRNA targeting exon 7. Additional synonymous mutations to remove EcoRV, BglII, KpnI, HindIII, and XbaI sites were also introduced. The myc-RAP80 cDNA was cloned into pcDNA5/FRT/TO at BamHI-EcoRV. The SIM binding mutant F40A/V41A/I42A was generated by SDM (GenScript). Human Abraxas and BRCC36 cDNA have synonymous mutations to silence restriction sites and render siRNA resistance and were cloned into pcDNA5/FRT/TO using KpnI - XhoI. Mutations in Abraxas and BRCC36 were introduced by SDM (GenScript).

### SIM-peptide pull-down assay

U2OS were plated at  $1 \times 10^6$  cells in 10 cm<sup>2</sup> plates and transfected with 5  $\mu$ g pcDNA5 FRT TO-6xHis-HA SUMO4 or pcDNA5 FRT TO-6xHis-HA SUMO4-QFI-A and treated with 4  $\mu$ g/ml doxycycline for a 48-hour incubation. U2OS cells were lysed in ice-cold RIPA buffer supplemented with protease inhibitors (Roche) and phosphatase inhibitors (Roche). Samples were sonicated at 10 kHz for 2x10 seconds with recovery followed by centrifugation at 14,000g at 4°C for 5 minutes. Magna-bind Streptavidin beads (Thermo Scientific) were washed in TBST and blocked with 20% BSA (TBST) for 2 hours at 4°C with agitation. Each pull-down condition included U2OS lysate, 15  $\mu$ l streptavidin beads, and 10  $\mu$ g Biotin-SIM-peptides (PIAS1: Biotin-NKKVEIDLTDSSSDEEEEEE or SLX4: Biotin-LNEEDEVILLDSDEELE) subjected to agitation at 4°C overnight. Streptavidin pull-downs were then washed twice in RIPA buffer (protease and phosphatase inhibitors) and then boiled at 95°C in 4xlaemmli buffer. Samples were then centrifuged at 16,000g and analysed using western blots.

### Vinyl-sulfone labeling and turnover kinetics

Vinyl-sulfone labelling, U2OS cells plated on 10 cm<sup>2</sup> dishes were treated as indicated for 48 hr before pelleting in ice cold PBS and lysis in 1 mL of buffer (150 mM NaCl 10 mM HEPES pH 7.8, 10 mM KCl, 1.5 mM MgCl<sub>2</sub>, 340 mM Sucrose, 10% glycerol 0.2% NP40,

protease and phosphatase inhibitor cocktails) followed by sonication and clarification by centrifugation. HA-SUMO-VS (Biotechne) were diluted in PBS and added at a final concentration of 10 ng in a volume of 100  $\mu$ L for 20 min incubation at room temperature. Reactions were stopped by the addition of 6x Laemmli buffer and boiled. Turnover kinetics, for each condition, 2x10 cm<sup>2</sup> dishes of U2OS (1x10<sup>6</sup> cell) were plated, siRNA transfected and doxycycline-treated for 48 hr. Cells were pelleted in PBS control for each condition and were lysed in 1  $\mu$ L of buffer (250 mM NaCl, 10 mM HEPES pH 7.8, 10 mM KCl, 1.5 mM MgCl<sub>2</sub>, 340 mM Sucrose, 10% glycerol 0.2% NP40, protease and phosphatase inhibitor cocktails) containing 200 mM IAA. After vigorous mixing by pipette for 30 seconds, 150  $\mu$ L of the sample was added to 50  $\mu$ L of Laemmli buffer. For turnover, cells were lysed in buffer without IAA, mixed by pipetting and 150  $\mu$ L samples mixed at indicated times with Laemmli to stop deconjugation, samples were subsequently sonicated and boiled. Details of all antibodies, including concentrations used in this study can be found in the [Table S2](#) and [key resources table](#)

### Metaphase spreads

Cells were plated on 6 well plates 24 hr prior to irradiation at 2 or 3 Gy. The cells were allowed to recover for 24 hr followed by incubation with Karyomax (colcemid) (0.05  $\mu$ g/ml) for 16 h. Cells were trypsinized and pelleted at 300g for 5 minutes, followed by resuspension in 5 ml of ice-cold 0.56% KCl and incubated at 37°C for 15 min before pelleting at 300g was resuspended and fixed in 5 mL of fixative (ice-cold methanol: glacial acetic acid (3:1)). Fixative was removed, and 15  $\mu$ l of cell suspension was dropped onto alcohol cleaned slides. Slides were allowed to dry at least 24 hr and then stained with Giemsa solution (Sigma) diluted 1:20 for 20 min. Slide mounting was performed with Eukitt mounting media (Sigma).

### Purification of recombinant proteins

#### SUMO protein preparation

BL21(DE3) cells were transformed with pGEX-4T1-GST-ProSUMO3 or pGEX-6P1-GST-SUMO4. Single colonies were used to inoculate 40 ml LB (100  $\mu$ g/ml ampicillin) and incubated at 37°C. This starter culture was used to inoculate 2-liter LB cultures (100  $\mu$ g/ml ampicillin) and incubated at 37°C/ 180 rpm to OD<sub>595</sub> 0.6-0.8. The incubation temperature was reduced to 18°C and 0.5 mM IPTG was added to the cultures for 12-16 hours. BL21(DE3) cells were harvested by centrifugation at 5,000g/ 4°C for 10 minutes. Bacterial pellets were resuspended in ice-cold lysis buffer (20 mM Tris-HCl pH8, 130 mM NaCl, 1mM EDTA, 1% TritonX-100, 10% glycerol, 1 mM DTT, EDTA-free protease inhibitor (Roche)). The bacterial suspension was incubated with 0.5 mg/ml lysozyme for 30 minutes/ 4°C with agitation. 1U/ml DNase (ThermoFisher) was added and samples were sonicated at 20 kHz for 5x30s with 2-minute recovery periods. Samples were centrifuged at 48,000g/ 4°C for 30 minutes. The supernatant was combined with 250  $\mu$ l Glutathione Sepharose 4B beads (Cytiva) at 4°C for 2 hours with agitation. Samples were centrifuged at 1,000g/4°C/10 minutes and beads were washed thrice with 5 ml lysis buffer and once with 5 ml cleavage buffer. GST-ProSUMO3 purification involved thrombin cleavage buffer (20 mM Tris-HCl pH 8.4, 150 mM NaCl, 1.5 mM CaCl<sub>2</sub>), and GST-SUMO4 purification required PreScission protease cleavage buffer (50 mM Tris-HCl pH 7, 150 mM NaCl, 1 mM EDTA, 1mM DTT) due to a vulnerable thrombin cleavage site unique to SUMO4. GST beads were suspended in 500  $\mu$ l cleavage buffer and as appropriate 16 U thrombin or 30 U PreScission protease were added for 16 hours/ 4°C with agitation. Samples were centrifuged at 1,000g/ 4°C/ 3 minutes, and the supernatant was isolated for centrifugation at 14,000g/ 4°C for 20 minutes. The supernatant was passed through a 0.45  $\mu$ m filter before size-exclusion chromatography (SEC) using an AKTA pure™ (UNICORN™ software) Superdex200 Increase 10/300 GL column equilibrated in 20 mM Hepes pH 7.5, 100 mM NaCl, 0.5 mM TCEP: 0.5 ml fractions collected. Eluted fractions corresponding with an increased UV<sub>280</sub> trace were analysed by SDS-PAGE stained with InstantBlue (Lubioscience). Pure SUMO protein fractions were pooled and stored at -80°C.

#### SAE1:SAE2 and RanGAP1(aa398-587) preparation

BL21 (DE3) were transformed with pET28a-His-hAos1, pET28b-hUba2-His, or pET23a-His-hRanGAP1tail. Single colonies were picked to inoculate 40 ml LB and grown at 37°C. Starter cultures were used to 10 ml starter cultures used to inoculate each litre LB (50  $\mu$ g/ml kanamycin or 100  $\mu$ g/ml ampicillin) and grown at 37°C/180 rpm to OD<sub>595</sub> ~0.6. Protein overexpression was induced with 1 mM IPTG for SAE1 and SAE2 at 25°C/6 hours and RanGAP1-tail(aa398-587) at 37°C/4 hours. BL21(DE3) cells were harvested by centrifugation at 5,000g/4°C/10 minutes and bacterial pellets were resuspended in 10 ml cold lysis buffer (20 mM Tris/HCl pH 8.0, 300 mM NaCl, 10 mM imidazole, 2 mM  $\beta$ -mercaptoethanol, protease inhibitor). Separately overexpressed SAE1 and SAE2 were combined here. 0.5 mg/ml lysozyme was added and incubated for 30 minutes/4°C/rolling. 1 U/ml DNase was added before sonication at 5x30s at 20 kHz with 2-minute recovery – all on ice. Samples were centrifuged at 48,000xg/4°C/30 minutes and the supernatant was filtered through a 0.45  $\mu$ m PES membrane (Millex). His-tagged protein lysates were combined with 1 ml nickel beads (Sigma) and incubated at 4°C/2 hours/agitation. Samples were then centrifuged at 1,000g/4°C/10 mins to pellet nickel beads which were resuspended in 10 ml wash buffer (20 mM Tris/HCl pH 8.0, 300 mM NaCl, 50 mM imidazole, 1 mM  $\beta$ -mercaptoethanol, protease inhibitor) ahead of centrifugation as before. Nickel beads resuspended in 5 ml elution buffer (20 mM Tris/HCl pH 8.0, 300 mM NaCl, 500 mM imidazole, 1 mM  $\beta$ -mercaptoethanol, protease inhibitor) and centrifuged as before; supernatant extracted and pushed through 0.45  $\mu$ m PES filter. This protein suspension was run using an AKTA pure™ (UNICORN™ software) on a HiLoad 16/600 Superdex200 pg column equilibrated with 20 mM Hepes pH 7.5, 100 mM NaCl, 0.5 mM TCEP buffer: 2 ml fractions collected. Fractions corresponding with a UV<sub>280</sub> peak were analyzed by SDS-PAGE stained with InstantBlue. Fractions containing the purest SAE1:SAE2 or RanGAP1(aa398-587) were pooled and stored at -80°C.

### **Ubc9 purification**

BL21 (DE3) were transformed with pET23a-Ubc9. A single colony was picked to inoculate a 40 ml LB (100 µg/ml ampicillin) started culture, which was grown at 37°C and in turn used to inoculate 2 L LB (100 µg/ml ampicillin). The cultures were grown to an OD<sub>595</sub> of 0.6 and Ubc9 overexpression was induced with 1 mM IPTG at 37°C for 4 hours. Cells were harvested by centrifugation at 5,000g/4°C/10 minutes and bacterial pellets were resuspended in 10 ml cold lysis buffer (50 mM Na-phosphate pH 6.5) before lysis using a C3 Emulsiflex. The cell lysate was centrifuged at 48,000g/4°C/30 minutes and the supernatant was filtered through a 0.45 µm PES membrane. The Ubc9 lysate was applied to an SP-sepharose column and latterly washed using the lysis buffer. Ubc9 was eluted from the column using 20 ml Ubc9 elution buffer (50 mM Na-phosphate pH 6.5, 300 mM NaCl, 1 mM DTT, plus cOmplete protease inhibitor) and 1.5 ml fractions were collected. Fractions with the greatest quantity and purity of Ubc9 were pooled and purified by SEC through a Superdex75 equilibrated in transport buffer (20 mM Hepes pH 7.3, 110 mM potassium acetate, 1 mM EGTA, 1 mM DTT, 1 cOmplete protease inhibitor): 4 ml fractions collected. Fractions constituting UV<sub>280</sub> peak were analyzed by 15% SDS-PAGE and Instantblue stain. Pure Ubc9 protein fractions were pooled and stored at -80°C.

### **Chemical cross-linking interaction analysis**

SEN1c (5 µM), SUMO2 (40 µM) and/or SUMO4 (40 µM), were incubated with or without homofunctional NHS-ester crosslinker, bis [sulfosuccinimidyl] suberate (BS<sup>3</sup>) at 800 µM (20 x molar excess to SUMO isoforms). For investigation of the influence of a SIM patch; SEN1c (5 µM), SUMO4 (40 µM), SLX4 peptides WT and mutant peptides at varying concentrations (30, 60 and 120 µM) were all incubated with BS<sup>3</sup> (800 µM). Peptide sequence information can be found in the KRT. All reactions were conducted in PBS for 30 minutes at room temperature before quenching with the addition of 2 x Laemmli buffer for 15 minutes at room temperature. Samples were boiled at 95°C for 5 minutes and run on 15% SDS-PAGE and visualised using Coomassie stain or SYPRO ruby.

### **ProSUMO3 maturation assay**

200 nM SENP1 (catalytic subunit; R&D systems) and 5 µM recombinant SUMO4 (rSUMO4) were pre-incubated in 50 mM Tris-HCl pH 8, 20 mM NaCl, and 5 mM DTT at 30°C for 30 minutes prior to the addition of 5 µM proSUMO3 in a 20 µl reaction volume. 200 nM SENP1 was pre-incubated +/- 5 µM rSUMO4 at 30°C for 30 minutes prior to the addition of 5 µM Pro-SUMO3 and incubated for the further indicated times before processing and immunoblotting for SUMO2/3. Reactions were terminated by the addition of 20 µl 4xLaemmli buffer and boiling at 95°C for 10 minutes. Samples were analyzed by western blots using SUMO2/3 antibodies.

### **DiSUMO2 cleavage assay**

25 nM SENP1 and 125 nM rSUMO4 were pre-incubated in the same buffer at 30°C for 30 minutes prior to the addition of 12.6 µM diSUMO2 (R&D systems) in a 20 µl reaction volume. The reactions were incubated for the indicated times before processing and immunoblotting for SUMO2/3. Reactions were terminated by the addition of 20 µl 4xLaemmli buffer and boiling at 95°C for 10 minutes. Samples were analyzed by western blots using SUMO2/3 antibodies.

### **HisRanGAP1(aa398-587)-SUMO1 deSUMOylation assay**

HisRanGAP1(aa398-587)-SUMO1 was prepared by combining 200 nM SAE1:SAE2, 500 nM Ubc9, 20 µM HisRanGAP1(aa398-587), 20 µM SUMO1, and 5 mM ATP in 20 mM Hepes pH 7.5, 50 mM NaCl, and 5 mM MgCl<sub>2</sub>, incubated at 37°C overnight before the addition of 2 µM 2-D08 (Ubc9 inhibitor). HisRanGAP1(aa398-587)-SUMO1 deSUMOylation assays involved preincubation of 25 nM SENP1 with 1 µM rSUMO4 for 30 minutes at 30°C in the same buffer and prior to the addition of 1 µM HisRanGAP1(aa398-587)-SUMO1 for a 20 µl reaction mix. Reactions were terminated by adding 20 µl 4x Laemmli buffer and incubation at 95°C for 10 minutes. Samples were analyzed by western blots using polyHis antibody.

## **QUANTIFICATION AND STATISTICAL ANALYSIS**

### **Statistics**

Statistical analysis was by two-tailed Student's t-test unless otherwise stated. \**p*<0.05, \*\**p*<0.01, \*\*\**P*<0.005 \*\*\*\* *P*<0.0001. All centre values are given as the mean and all error bars are standard error about the mean (S.E.M.). The statistical details of experiments can be found in the figure legends. All statistical differences were calculated using GraphPad Prism software (v7.7e, GraphPad Software Inc., USA). Images were analyzed using ImageJ software.<sup>85,87</sup>